ETH
Eidgenössische Technische Hochschule Zürich
Swiss Federal Institute of Technology Zurich

Seminar for Applied Mathematics SAM

hp-FEM for reaction-diffusion equations. II: Robust exponential convergence for multiple length scales in corner domains

L. Banjai and J.M. Melenk and Ch. Schwab

Research Report No. 2020-28

May 2020
Latest revision: December 2021

Seminar für Angewandte Mathematik
Eidgenössische Technische Hochschule
CH-8092 Zürich
Switzerland

Funding: Austrian Science Fund (FWF) project F 65; Swiss National Science Foundation.

IMA Journal of Numerical Analysis (2021) Page 1 of 40
doi:10.1093/imanum/drn000

hp-FEM for reaction-diffusion equations. II: Robust exponential convergence for multiple length scales in corner domains. †

Lehel Banjai‡ and Jens M. Melenk§ and Christoph Schwab¶

[Received on 1 December 2021]

In bounded, polygonal domains $\Omega \subset \mathbb{R}^2$ with Lipschitz boundary $\partial\Omega$ consisting of a finite number of Jordan curves admitting analytic parametrizations, we analyze *hp*-FEM discretizations of linear, second order, singularly perturbed reaction diffusion equations on so-called *geometric boundary layer meshes*. We prove, under suitable analyticity assumptions on the data, that these *hp*-FEM afford exponential convergence in the natural "energy" norm of the problem, as long as the geometric boundary layer mesh can resolve the smallest length scale present in the problem. Numerical experiments confirm the robust exponential convergence of the proposed *hp*-FEM.

Keywords: anisotropic *hp*–refinement, geometric corner refinement, exponential convergence.

1. Introduction

The need for accurate numerical approximations of solutions to singularly perturbed partial differential equations in nonsmooth domains arises in a wide range of applications, e.g., in structural mechanics in the theory of plates and shells as well as fluid mechanics in vicous, incompressible flow. Typically, these solutions feature singularities near regions of nonsmoothness of the geometry as well as boundary layers induced by the singular perturbation nature of the equation. These boundary layers occur frequently on multiple length scales. We mention dimensionally reduced models of curved thin solids ("shells") in so-called "bending-dominated" states (see, e.g., Chaussade-Beaudouin *et al.* (2017) and the references there for a detailed discussion of possible length scales), and linear, elliptic reaction-diffusion boundary value problems that result from implicit time-discretizations of parabolic evolution equations and, more recently, from discretizations of fractional powers of elliptic operators (see, e.g., Banjai *et al.* (2019); Melenk & Rieder (2021) and the references there). Advection-diffusion problems often have layers with complicated structure in particular near points where the boundary becomes characteristic. Interaction of corner singularities and layers arise also in electromagnetics in so-called eddy-current models (where the small parameter is a complex number) (see, e.g., Buret *et al.* (2012) and the references there).

High order methods for singularly perturbed problems can lead to exponential convergence on specially designed meshes to capture boundary layers of a given scale, Schwab & Suri (1996); Melenk &

†The research of JMM was supported by the Austrian Science Fund (FWF) project F 65. Work performed in part while CS was visiting the Erwin Schrödinger Institute (ESI) in Vienna in June-August 2018 during the ESI thematic period "Numerical Analysis of Complex PDE Models in the Sciences". Research of CS supported in part by the Swiss National Science Foundation.

‡Maxwell Institute for Mathematical Sciences, School of Mathematical & Computer Sciences, Heriot-Watt University, Edinburgh EH14 4AS, UK (l.banjai@hw.ac.uk).

§Institut für Analysis und Scientific Computing, Technische Universität Wien, A-1040 Vienna, Austria (melenk@tuwien.ac.at).

¶Seminar for Applied Mathematics, ETH Zürich, ETH Zentrum, HG G57.1, CH8092 Zürich, Switzerland (christoph.schwab@sam.math.ethz.ch).

Schwab (1998); Melenk (1997); Melenk & Schwab (1999); Melenk (2002) and the references there. These references focus on boundary layers on a single scale on smooth geometries. In nonsmooth geometries, the interaction of corner singularities and layers is highly non-trivial and correspondingly the design of meshes or numerical methods is challenging. In the present work, we propose *geometric boundary layer meshes* (GBLM) that are geometrically refined towards both corners and edges of the domain. Such meshes are capable to resolve boundary layers of any length scale down to a minimal one that depends the refinement level of the GBLM. The geometric refinement towards corners also allows for simultaneously resolving corner singularities, typical of elliptic problems in corner domains.

For analysis purposes, our GBLM are constructed in a patch-based fashion in that the actual mesh is defined as the push-forwards of finitely many reference refinement configurations. Our convergence analysis focuses on the approximation of typical corner layers and boundary layers of any length scale on these patches and could be applied whenever the solution structure in terms of such components is available. Such structural information is made available in Melenk (2002) for a singularly perturbed scalar reaction-diffusion problem in polygons. Based on that detailed regularity analysis, we are able to provide a full convergence analysis of the hp-FEM for that scalar singularly perturbed model problem in polygons and show exponential convergence on the GBLM proposed here. Thus, the present work extends in the scalar reaction-diffusion case the hp-error analysis of Part I, Melenk & Schwab (1998), to polygons. However, the scope of the mesh design principles presented here is wider as they are applicable to more complex singularly perturbed PDEs with multiple scales, see Arnold & Falk (1996); Gerdes *et al.* (1998); Chaussade-Beaudouin *et al.* (2017); Gie *et al.* (2018) and the references there. We underline the success of the GBLM with a numerical example from fractional diffusion in polygons, where the numerical solution involves solving a collection of *local* singularly perturbed reaction-diffusion problems with a wide range of boundary layer length scales.

1.1 *Model reaction-diffusion problem*

In a bounded domain $\Omega \subset \mathbb{R}^2$, which is assumed to be scaled to unit size, and for a parameter $0 < \varepsilon \leqslant 1$, we consider the hp-FE approximation of the *model reaction-diffusion Dirichlet problem*

$$-\varepsilon^2 \nabla \cdot (A(\mathbf{x})\nabla u_\varepsilon) + c(\mathbf{x}) u_\varepsilon = f \quad \text{in } \Omega, \qquad u_\varepsilon = 0 \quad \text{on } \partial\Omega. \tag{1.1}$$

We assume

$$\begin{array}{l} A,\, c,\, f \text{ analytic on } \overline{\Omega}, \text{ independent of } \varepsilon, \\ A \text{ symmetric, positive definite uniformly in } \overline{\Omega},\ c \geqslant c_0 > 0 \text{ on } \overline{\Omega}. \end{array} \tag{1.2}$$

To design $H^1_0(\Omega)$-conforming, hp-FE approximations of the solutions $\{u_\varepsilon : 0 < \varepsilon \leqslant 1\}$ of (1.1) under the analyticity assumptions (1.2) which converge exponentially in the ε-dependent energy norm $\|\circ\|_{\varepsilon,\Omega}$ given by

$$\|v\|^2_{\varepsilon,\Omega} := \varepsilon^2 \|\nabla v\|^2_{L^2(\Omega)} + \|v\|^2_{L^2(\Omega)}, \quad v \in H^1(\Omega), \tag{1.3}$$

is the purpose of the present paper. We prove in particular in Theorem 4.1 a *robust exponential convergence error bound*, i.e., all constants in the exponential convergence bound do not depend on $\varepsilon > 0$.

We again emphasize that we consider (1.1) for illustration. The scope of the robust exponential hp convergence rate bounds below extends well beyond (1.1) to more complex, singularly perturbed PDE such as those in Arnold & Falk (1996); Gerdes *et al.* (1998); Chaussade-Beaudouin *et al.* (2017).

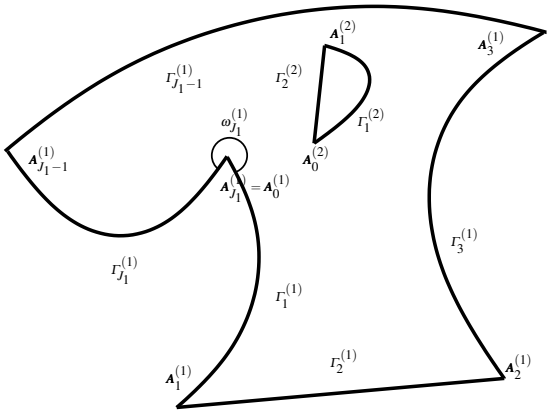

FIG. 1. Example of a curvilinear polygon Ω.

1.2 *Geometric Preliminaries*

In (1.2), the domain $\Omega \subset \mathbb{R}^2$ is a curvilinear polygonal domain, schematically depicted in Fig. 1. Specifically, the boundary $\partial\Omega$ is assumed to consist of $J \in \mathbb{N}$ closed curves $\Gamma^{(i)}$. Each curve $\Gamma^{(i)}$ in turn is assumed to be partitioned into finitely many open, disjoint, *analytic arcs* $\Gamma_j^{(i)}$, in the sense that there are numbers $J_i \in \mathbb{N}$ such that

$$\overline{\Gamma^{(i)}} = \bigcup_{j=1}^{J_i} \overline{\Gamma_j^{(i)}}\,, \quad i = 1,\dots,J\,.$$

Here, *analytic arcs* $\Gamma_j^{(i)}$ admit *nondegenerate, analytic parametrizations*, i.e.,

$$\Gamma_j^{(i)} = \left\{ \mathbf{x}_j^{(i)}(\theta) | \theta \in (0,1) \right\}\,, \quad i = 1,...,J, \quad j = 1,...,J_i\,.$$

with the coordinate functions $x_j^{(i)}$, $y_j^{(i)}$ of $\mathbf{x}_j^{(i)}(\theta) = (x_j^{(i)}(\theta), y_j^{(i)}(\theta))$ assumed to be (real) analytic functions of $\theta \in [0,1]$ and such that

$$\min_{\theta\in[0,1]} \left\{ \left| \frac{d}{d\theta} x_j^{(i)}(\theta) \right|^2 + \left| \frac{d}{d\theta} y_j^{(i)}(\theta) \right|^2 \right\} > 0, \quad j = 1,...,J_i, \quad i = 1,...,J\,.$$

We denote $\partial\Gamma_j^{(i)} = \{\boldsymbol{A}_{j-1}^{(i)}, \boldsymbol{A}_j^{(i)}\}$ where $\boldsymbol{A}_{j-1}^{(i)} = \mathbf{x}_j^{(i)}(0)$ and $\boldsymbol{A}_j^{(i)} = \mathbf{x}_j^{(i)}(1)$. For each boundary component $\Gamma^{(i)}$, we enumerate $\{\boldsymbol{A}_j^{(i)}\}_{j=1}^{J_i}$ cyclically, counterclockwise by indexing with j modulo J_i, thereby identifying in particular $\boldsymbol{A}_j^{(i)} := \boldsymbol{A}_{j+J_i}^{(i)}$. The interior angle at $A_j^{(i)}$ is denoted $\omega_j^{(i)} \in (0, 2\pi)$. For notational simplicity, we assume henceforth that $J = 1$, i.e., $\partial\Omega$ consists of a single component of connectedness. We write $\boldsymbol{A}_j = \boldsymbol{A}_j^{(1)}$, Γ_j for $\Gamma_j^{(1)}$, $x_j = x_j^{(1)}$, $y_j = y_j^{(1)}$. Then, in a vicinity of any point $x \in \partial\Omega$, a curvilinear polygon Ω is *analytically diffeomorphic* to either a half-space, or to a plane sector with vertex situated at the origin.

1.3 *Contributions*

The principal contribution of the present paper is the development of the GBLM in Section 2.3 and the proof that these meshes allow to approximate boundary layers as well as corner layers at an exponential rate in Section 3. As an important application, we show in Section 4 *robust, exponential convergence of a class of hp-FEM approximations* of the singular perturbation problem (1.1) under the analyticity assumptions (1.2), in curvilinear polygons Ω as described in Section 1.2. The convergence proof in Sections 3 and 4 is done under a *scale resolution condition* that corresponds, roughly speaking, to the hp-FE partitions resolving the shortest length scale that occurs in the solution u_ε, and it is strongly based on *parameter-explicit, analytic regularity results* for the parametric solution family $\{u_\varepsilon : 0 < \varepsilon \leqslant 1\} \subset H^1_0(\Omega)$ of (1.1), which were obtained by one of the authors in Melenk (2002). Importantly, and distinct from earlier work on robust exponential hp-FE convergence for (1.1), a *patch-based convergence proof* is developed which also enables an algorithmic, patchwise-structured anisotropic mesh specification, described in Section 2, which is applicable in domains Ω of the generality admitted in Section 1.2. As we show in numerical experiments in Section 5, the mesh generator Netgen Schöberl (1997) does produce automatically, i.e., without "expert pruning", anisotropic, geometric meshes in Ω with the required boundary and corner refinement capable to deliver robust exponential convergence.

1.4 *Outline of this paper*

In Section 2, we introduce the geometric mesh families in Ω that underlie our robust exponential convergence results. The meshes require concurrent anisotropic geometric partitions of Ω towards the boundary $\partial\Omega$ and isotropic geometric refinement towards the corners $\boldsymbol{A}_j$. We define these meshes in a macro-element fashion based on an initial, coarse regular partition of the physical domain Ω into a *macro-triangulation* consisting of a *regular, finite, and fixed partition of the physical domain* Ω that is described in Section 2.1. Its elements will be referred to as *(macro) patches* and are assumed to be images of a finite number of quadrilateral reference patches under *analytic patch maps*. The reference patches are key in ensuring robust exponential convergence rate bounds of our hp-FEM approximation. Following earlier work Melenk (1997); Melenk & Schwab (1999); Melenk (2002), we consider so-called *geometric boundary layer meshes*, denoted by $\mathscr{T}^{L,n}_{geo,\sigma}$. We introduce these in Def. 2.2. Unlike the so-called "two-element" meshes considered earlier in Schwab *et al.* (1998a,b), which are designed to approximate only a single small scale in a robust way, the presently considered geometric boundary layer meshes afford robust exponential convergence rates of hp-FEM also in the presence of multiple physical length scales. This situation arises in a number of applications (e.g., Chaussade-Beaudouin *et al.* (2017); Banjai *et al.* (2019)). Section 2.3 introduces the geometric boundary layer mesh, first on the reference patches, and then in Section 2.4 in curvilinear polygons.

Section 3 is devoted to the polynomial approximation of functions on geometric boundary layer meshes. The approximation is based on Gauss-Lobatto interpolation operators in the reference triangle, indicated by $\triangle$, and in the reference square, indicated by $\square$, in Section 3.1. These are then assembled into (nodal) patch approximation operators on the geometric boundary layer patches in Section 3.2. Then, the robust hp-approximation of corner singularities and boundary layer functions is proved. These functions are the key solution components of singularly perturbed problems in polygons such as the model problem (1.1).

Section 4 assembles the patch hp-approximation results and interpolants into a global approximation operator, and presents the main result of this paper: robust exponential convergence rate bounds for the global hp-interpolation of the solution of (1.1) assembled from the patch approximations.

Section 5 presents several illustrative numerical experiments in polygons, which underline the theoretical results. Besides singular perturbation problems with single scales we include an example from

fractional diffusion whose numerical treatment naturally leads to a collection of singularly perturbed problems with multiple scales. All our numerical examples are based on *hp*-meshes that are furnished by the automated mesh generation procedure Netgen Schöberl (1997) to make the point that the somewhat technical construction of geometric boundary layer meshes is, in principle, available and feasible automatically. Appendix A contains proofs of auxiliary results on analytic regularity estimates under analytic changes of variables. Appendix B collects (mostly known) results on univariate polynomial approximation for convenient reference in the main text.

1.5 *Notation*

We employ standard notation for Sobolev spaces. Constants C, γ, $b > 0$ may be different in different instances. However, they will be independent of parameters of interest such as $\varepsilon \in (0,1]$, the polynomial degree q, and the element under consideration. The notation $\nabla^n u$ stands for the collection of all partial derivatives of order n and $|\nabla^n u|^2 = \sum_{|\alpha|=n} \frac{n!}{\alpha!} |D^\alpha u|^2$. Points in $\mathbb{R}^2$ will be denoted depending on the context as either $\mathbf{x} = (x,y)$ (physical domain) or $\widetilde{\mathbf{x}} = (\widetilde{x},\widetilde{y})$ (patch domains) or $\widehat{\mathbf{x}} = (\widehat{x},\widehat{y})$ (reference domains). We abbreviate $\{\widetilde{x}=0\}$, $\{\widetilde{y}=0\}$, and $\{\widetilde{x}=\widetilde{y}\}$ for the line segments $\{\widetilde{\mathbf{x}} = (0,\widetilde{y}) \,|\, 0 < \widetilde{y} < 1\}$, $\{\widetilde{\mathbf{x}} = (\widetilde{x},0) \,|\, 0 < \widetilde{x} < 1\}$, and $\{\widetilde{\mathbf{x}} = (\widetilde{x},\widetilde{y}) \,|\, 0 < \widetilde{x} = \widetilde{y} < 1\}$, respectively. We write $\{\widetilde{y} \leqslant \widetilde{x}\}$ for $\{\widetilde{\mathbf{x}} = (\widetilde{x},\widetilde{y}) \,|\, 0 < \widetilde{y} \leqslant \widetilde{x} < 1\}$. The origin will be denoted $\mathbf{0} = (0,0)$. The reference square and triangle are $\widehat{S} := (0,1)^2$ and $\widehat{T} := \{(\widehat{x},\widehat{y}) \,|\, 0 < \widehat{x} < 1, 0 < \widehat{y} < \widehat{x}\}$. The region covered by the reference patch will be denoted $\widetilde{S} := \widehat{S} = (0,1)^2$. It will be convenient to introduce $\widetilde{T} := \widehat{T}$ and set $T^{\text{flip}} := \widetilde{S} \setminus \overline{\widetilde{T}}$. We denote the space of polynomials of total degree q by $\mathbb{P}_q = \operatorname{span}\{x^i y^j \,|\, 0 \leqslant i+j \leqslant q\}$; the tensor product space $\mathbb{Q}_q$ is $\mathbb{Q}_q = \operatorname{span}\{x^i y^j \,|\, 0 \leqslant i,j \leqslant q\}$.

2. Macro triangulation. Geometric boundary layer mesh (GBLM)

Our robust exponentially convergent *hp* approximation is based on so-called *geometric boundary layer meshes*, denoted by $\mathscr{T}^{L,n}_{geo,\sigma}$. To facilitate our error analysis, the $\mathscr{T}^{L,n}_{geo,\sigma}$ are generated as push-forwards of a small number of so-called *reference patches*, which are partitions of $\widetilde{S}$, under the *patch maps*. The images of $\widetilde{S}$ under the patch maps form a (coarse) *macro triangulation* of Ω satisfying some minimal conditions, which are described in Section 2.1. This concept was also used in the context of *hp*-FEM for singular perturbations in (Melenk, 2002, Sec. 3.3.3) and in Melenk & Xenophontos (2016); Faustmann & Melenk (2017).

2.1 *Macro triangulations*

We assume given a *fixed macro-triangulation* $\mathscr{T}^{\mathscr{M}} = \{K^{\mathscr{M}} \,|\, K^{\mathscr{M}} \in \mathscr{T}^{\mathscr{M}}\}$ of Ω consisting of curvilinear quadrilaterals $K^{\mathscr{M}}$ with bijective element maps $F_{K^{\mathscr{M}}} : \widetilde{S} \to K^{\mathscr{M}}$ that are analytic in $\overline{\widetilde{S}}$ and that in addition satisfy the usual compatibility conditions. I.e., the partition $\mathscr{T}^{\mathscr{M}}$ does not have hanging nodes and, for any two distinct elements $K_1^{\mathscr{M}}, K_2^{\mathscr{M}} \in \mathscr{T}^{\mathscr{M}}$ that share an edge e, their respective element maps induce compatible parametrizations of e (cf., e.g., (Melenk, 2002, Def. 2.4.1) for the precise conditions).

Each element of the fixed macro-triangulation $\mathscr{T}^{\mathscr{M}}$ is further subdivided according to one of the refinement patterns in Definition 2.1 (see also (Melenk, 2002, Sec. 3.3.3) or Faustmann & Melenk (2017)). The actual triangulation is then obtained by transplanting refinement patterns on the square reference patch $\widetilde{S}$ into the physical domain Ω by the element maps $F_{K^{\mathscr{M}}}$ of the macro-triangulation resulting in the *physical triangulation* $\mathscr{T}$. For any element $K \in \mathscr{T}$, the element maps $F_K : \widehat{K} \to K$ are then concatenations of affine maps $A_K : \widehat{K} \to \widetilde{K}$, which realize the mapping from $\widehat{K} \in \{\widehat{S},\widehat{T}\}$ to the

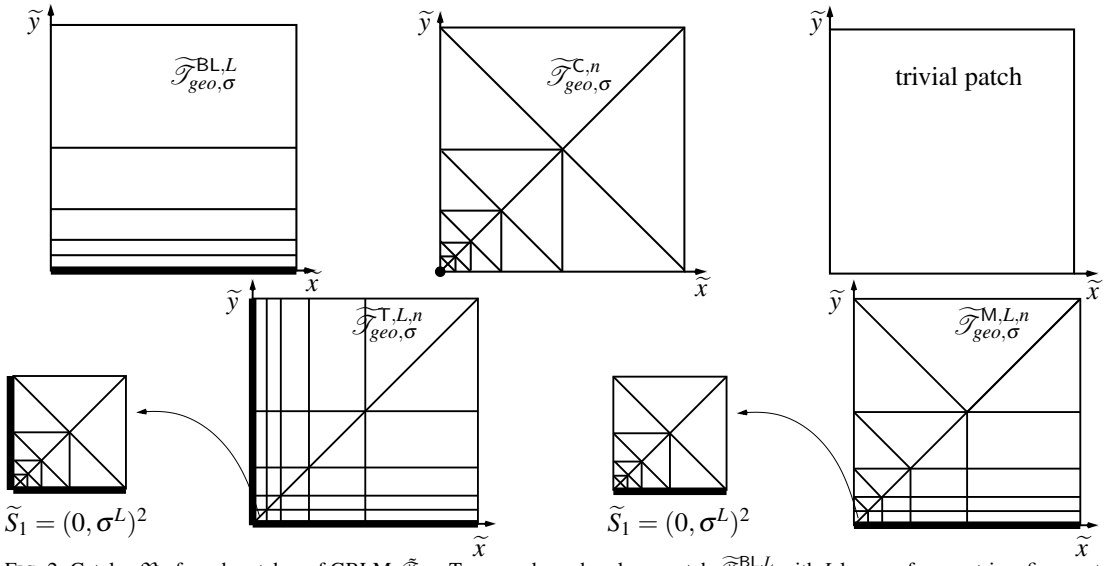

FIG. 2. Catalog $\mathfrak{P}$ of mesh patches of GBLM $\widetilde{\mathscr{T}}_{geo}$. Top row: boundary layer patch $\widetilde{\mathscr{T}}^{\mathsf{BL},L}_{geo,\sigma}$ with L layers of geometric refinement towards $\{\widetilde{y}=0\}$; corner patch $\widetilde{\mathscr{T}}^{\mathsf{C},n}_{geo,\sigma}$ with n layers of geometric refinement towards $(0,0)$; trivial patch. Bottom row: tensor patch $\widetilde{\mathscr{T}}^{\mathsf{T},L,n}_{geo,\sigma}$ with n layers of isotropic geometric refinement towards $(0,0)$ and L layers of anisotropic geometric refinement towards $\{\widetilde{x}=0\}$ and $\{\widetilde{y}=0\}$; mixed patch $\widetilde{\mathscr{T}}^{\mathsf{M},L,n}_{geo,\sigma}$ with L layers of refinement towards $\{y=0\}$ and n layers of refinement towards $(0,0)$. Geometric entities shown in boldface indicate parts of $\partial\widetilde{S}$ that are mapped to $\partial\Omega$. Patch meshes are transported into the curvilinear polygon Ω shown in Fig. 1 via analytic patch maps $F_{K^{\mathscr{M}}}$.

elements in the patch refinement pattern, and the analytic patch maps $F_{K^{\mathscr{M}}}$. That is, the element maps have the form $F_K = F_{K^{\mathscr{M}}} \circ A_K$ for an affine A_K. Throughout the article, we will denote by $\widehat{K} \in \{\widehat{S},\widehat{T}\}$ the reference element corresponding to an element K of a triangulation, and we will denote by $\widetilde{K}$ the elements of the triangulation of the reference patterns. Points in the reference patch $\widetilde{S}$ are denoted $\widetilde{\mathbf{x}} = (\widetilde{x},\widetilde{y}) \in \widetilde{S}$; variables (x,y) are employed to indicate points in Ω, and $\widehat{\mathbf{x}} = (\widehat{x},\widehat{y})$ are used for points of the reference square $\widehat{S} = (0,1)^2$ and reference triangle $\widehat{T} = \{(\widehat{x},\widehat{y}) \,|\, 0 < \widehat{y} < \widehat{x} < 1\}$.

2.2 *Refinement patterns in the reference configuration (patch catalog $\mathfrak{P}$)*

The admissible *patch refinement patterns* are collected in a catalog $\mathfrak{P}$ and are depicted in Fig. 2. They are based on geometric refinement towards a vertex and/or an edge; the parameter L controls the number of layers of refinement towards an edge whereas the natural number $n \geqslant L$ measures the number of geometric refinements towards vertices.

DEFINITION 2.1 (catalog $\mathfrak{P}$ of refinement patterns) Given $\sigma \in (0,1)$, L, $n \in \mathbb{N}_0$ with $n \geqslant L$ the catalog $\mathfrak{P}$ of admissible refinement patterns consists of the following patches:

1. The *trivial patch*: The reference square $\widetilde{S}$ is not further refined. The corresponding triangulation of $\widetilde{S}$ consists of the single element: $\widetilde{\mathscr{T}} = \{\widetilde{S}\}$.

2. The *geometric boundary layer patch* $\widetilde{\mathscr{T}}^{\mathsf{BL},L}_{geo,\sigma}$: $\widetilde{S}$ is refined anisotropically towards $\{\widetilde{y}=0\}$ into L elements as depicted in Fig. 2 (top left). The mesh $\widetilde{\mathscr{T}}^{\mathsf{BL},L}_{geo,\sigma}$ is characterized by the nodes $(0,0)$,

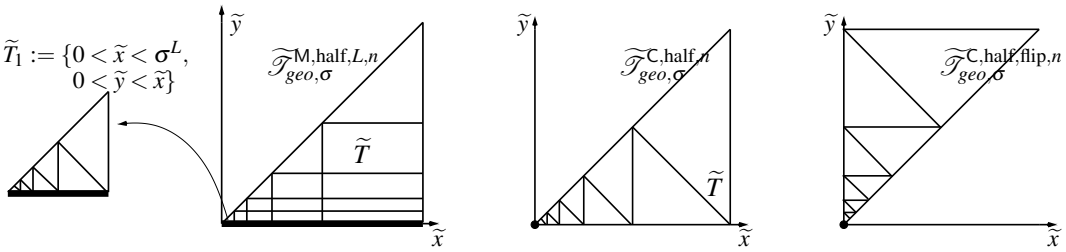

FIG. 3. From left to right: half-patches $\widetilde{\mathscr{T}}^{\mathsf{M},\mathrm{half},L,n}_{geo,\sigma}$, $\widetilde{\mathscr{T}}^{\mathsf{C},\mathrm{half},n}_{geo,\sigma}$, and $\widetilde{\mathscr{T}}^{\mathsf{C},\mathrm{half},\mathrm{flip},n}_{geo,\sigma}$. They are given by the elements of $\widetilde{\mathscr{T}}^{\mathsf{C},n}_{geo,\sigma}$ and $\widetilde{\mathscr{T}}^{\mathsf{M},L,n}_{geo,\sigma}$ below the diagonal $\{\widetilde{y} = \widetilde{x}\}$ and the mirror image of $\widetilde{\mathscr{T}}^{\mathsf{C},\mathrm{half},n}_{geo,\sigma}$ at the diagonal $\{\widetilde{y} = \widetilde{x}\}$.

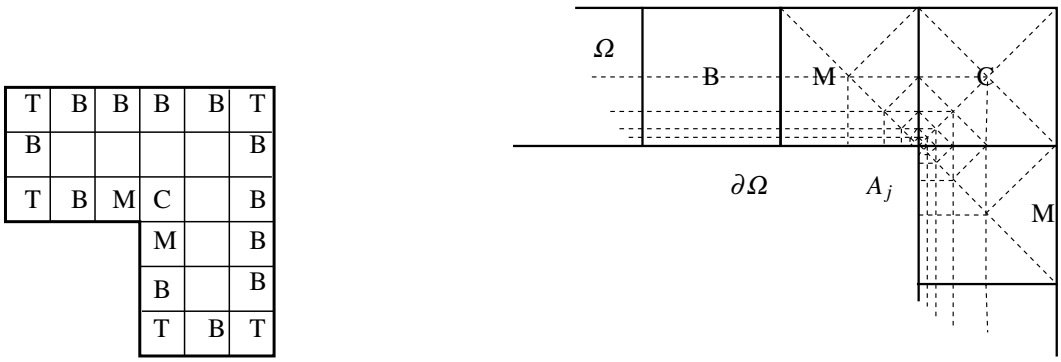

FIG. 4. Left panel: example of an L-shaped domain decomposed into 27 patches (T, B, M, C indicate tensor, boundary layer, mixed, corner patches; empty squares stand for trivial patches). Right panel: Zoom-in near the reentrant corner.

$(0,\sigma^i)$, $(1,\sigma^i)$, $i = 0,\dots,L$, and the corresponding rectangular elements generated by these nodes.

3. The *geometric corner patch* $\widetilde{\mathscr{T}}^{\mathsf{C},n}_{geo,\sigma}$: $\widetilde{S}$ is refined isotropically towards $(0,0)$ as depicted in Fig. 2 (top middle). Specifically, the reference geometric corner patch mesh $\widetilde{\mathscr{T}}^{\mathsf{C},n}_{geo,\sigma}$ in $\widetilde{S}$ with geometric refinement towards $(0,0)$ and n layers is given by triangles and based on the nodes $(0,0)$, and $(0,\sigma^i)$, $(\sigma^i,0)$, (σ^i,σ^i), $i = 0,1,\dots,n$.

4. The *tensor product patch* $\widetilde{\mathscr{T}}^{\mathsf{T},L,n}_{geo,\sigma}$: $\widetilde{S}$ is triangulated in $\widetilde{S}_1 := (0,\sigma^L)^2$ and $\widetilde{S}_2 := \widetilde{S} \setminus \widetilde{S}_1$ separately as depicted in Fig. 2 (bottom left). The triangulation of $\widetilde{S}_1$ is a scaled version of $\widetilde{\mathscr{T}}^{\mathsf{C},n-L}_{geo,\sigma}$ and based on the nodes $(0,\sigma^i)$, $(\sigma^i,0)$, $i = L,\dots,n$. The triangulation of $\widetilde{S}_2$ is based on the nodes (σ^i,σ^j), $i,\, j = 0,\dots,L$.

5. The *mixed patches* $\widetilde{\mathscr{T}}^{\mathsf{M},L,n}_{geo,\sigma}$: The triangulation consists of both anisotropic elements and isotropic elements as depicted in Fig. 2 (bottom right) and is obtained by triangulating the regions $\widetilde{S}_1 := (0,\sigma^L)^2$, $\widetilde{S}_2 := \big(\widetilde{S} \setminus \widetilde{S}_1\big) \cap \{\widetilde{y} \leqslant \widetilde{x}\}$, $\widetilde{S}_3 := \widetilde{S} \setminus (\widetilde{S}_1 \cup \widetilde{S}_2)$ separately. The set $\widetilde{S}_1$ is a scaled version of $\widetilde{\mathscr{T}}^{\mathsf{C},n-L}_{geo,\sigma}$ based on the nodes $(0,\sigma^i)$, $(\sigma^i,0)$, $i = L,\dots,n$. The triangulation of $\widetilde{S}_2$ is based on the nodes $(\sigma^i,0)$, (σ^i,σ^j), $0 \leqslant i \leqslant L$, $i \leqslant j \leqslant L$ and consists of rectangles and triangles, and only the triangles abut on the diagonal $\{\widetilde{x} = \widetilde{y}\}$. The triangulation of $\widetilde{S}_3$ consists of triangles only and is based on the nodes $(0,\sigma^i)$, (σ^i,σ^i), $i = 0,\dots,L$.

REMARK 2.1 We kept the catalog $\mathfrak{P}$ of admissible patch refinement patterns in Definition 2.1 small in order to reduce the number of cases to be discussed for the *hp*-FE error bounds. A larger number of refinement patterns provides greater flexibility in the mesh generation. In particular, the reference patch meshes of Def. 2.1 do not contain general quadrilaterals but only rectangles; this restriction is not essential but simplifies the *hp*-FE error analysis. Also certain types of anisotropic triangles (e.g., splitting anisotropic rectangles along the diagonal), which are altogether excluded in the present analysis, could be accommodated at the expense of additional technicalities.

The addition of the diagonal line in the reference corner, tensor, and mixed patches is done to be able to apply the regularity theory of Melenk (2002). It is likely not necessary in actual computations. We also mention that with additional constraints on the macro triangulation $\mathscr{T}^{\mathscr{M}}$ the diagonal line could be dispensed with in certain situations as is illustrated in Section 2.4. ∎

2.3 *Geometric boundary layer mesh*

The following definition of the geometric boundary layer mesh $\mathscr{T}^{L,n}_{geo,\sigma}$ formalizes the patchwise construction of meshes on Ω based on transplanting meshes of the reference configurations to Ω via the patch maps $F_{K^{\mathscr{M}}}$.

DEFINITION 2.2 (geometric boundary layer mesh $\mathscr{T}^{L,n}_{geo,\sigma}$ in Ω) Let $\mathscr{T}^{\mathscr{M}}$ be a fixed macro-triangulation consisting of quadrilaterals with analytic element maps that satisfy (Melenk, 2002, Def. 2.4.1).

Given $\sigma \in (0,1)$, L, $n \in \mathbb{N}_0$ with $n \geqslant L$, a regular mesh $\mathscr{T}^{L,n}_{geo,\sigma}$ in Ω is called a *geometric boundary layer mesh* if the following conditions are satisfied:

1. $\mathscr{T}^{L,n}_{geo,\sigma}$ is obtained by refining each element $K^{\mathscr{M}} \in \mathscr{T}^{\mathscr{M}}$ according to one of the refinement patterns given in Definition 2.1 using the given parameters σ, L, and n.
2. The resulting mesh $\mathscr{T}^{L,n}_{geo,\sigma}$ is a regular triangulation of Ω, i.e., it does not have hanging nodes. Since the element maps for the refinement patterns are assumed to be affine, this requirement ensures that the resulting triangulation satisfies (Melenk, 2002, Def. 2.4.1).

For each macro-patch $K^{\mathscr{M}} \in \mathscr{T}^{\mathscr{M}}$, exactly one of the following cases is possible:

3. $\overline{K^{\mathscr{M}}} \cap \partial\Omega = \emptyset$. Then the trivial patch is selected as the reference patch.
4. $\overline{K^{\mathscr{M}}} \cap \partial\Omega$ is a single point. Then two cases can occur:
   (a) $\overline{K^{\mathscr{M}}} \cap \partial\Omega = \{\boldsymbol{A}_j\}$ for a vertex $\boldsymbol{A}_j$ of Ω. Then the corresponding reference patch is the corner patch $\widehat{\mathscr{T}}^{\mathsf{C},n}_{geo,\sigma}$ with n layers of refinement towards $\mathbf{0}$. Additionally, $F_{K^{\mathscr{M}}}(\mathbf{0}) = \boldsymbol{A}_j$.
   (b) $\overline{K^{\mathscr{M}}} \cap \partial\Omega = \{\boldsymbol{P}\}$, where $\boldsymbol{P}$ is not a vertex of Ω. Then the refinement pattern is the corner patch $\widehat{\mathscr{T}}^{\mathsf{C},L}_{geo,\sigma}$ with L layers of geometric mesh refinement towards $\mathbf{0}$. Additionally, it is assumed that $F_{K^{\mathscr{M}}}(\mathbf{0}) = \boldsymbol{P} \in \partial\Omega$.
5. $\overline{K^{\mathscr{M}}} \cap \partial\Omega = \overline{e}$ for an edge e of $K^{\mathscr{M}}$ and neither endpoint of e is a vertex of Ω. Then the refinement pattern is the boundary layer patch $\widehat{\mathscr{T}}^{\mathsf{BL},L}_{geo,\sigma}$ and additionally $F_{K^{\mathscr{M}}}(\{\widetilde{y} = 0\}) \subset \partial\Omega$.
6. $\overline{K^{\mathscr{M}}} \cap \partial\Omega = \overline{e}$ for an edge e of $K^{\mathscr{M}}$ and exactly one endpoint of e is a vertex $\boldsymbol{A}_j$ of Ω. Then the refinement pattern is the mixed layer patch $\widehat{\mathscr{T}}^{\mathsf{M},L,n}_{geo,\sigma}$ and additionally $F_{K^{\mathscr{M}}}(\{\widetilde{y} = 0\}) \subset \partial\Omega$ as well as $F_{K^{\mathscr{M}}}(\mathbf{0}) = \boldsymbol{A}_j$.

7. Exactly two edges of a macro-element $K^{\mathscr{M}}$ are situated on $\partial\Omega$. Then the refinement pattern is the tensor patch $\widehat{\mathscr{T}}^{\mathsf{T},L,n}_{geo,\sigma}$. Additionally, it is assumed that $F_{K^{\mathscr{M}}}(\{\widetilde{y}=0\}) \subset \partial\Omega$, $F_{K^{\mathscr{M}}}(\{\widetilde{x}=0\}) \subset \partial\Omega$, and $F_{K^{\mathscr{M}}}(\mathbf{0}) = \boldsymbol{A}_j$ for a vertex $\boldsymbol{A}_j$ of Ω.

Finally, the following technical condition ensures the existence of certain meshlines:

8. For each vertex $\boldsymbol{A}_j$ of Ω, introduce a set of lines

$$\ell = \bigcup_{K^{\mathscr{M}}\,:\,\boldsymbol{A}_j \in \overline{K^{\mathscr{M}}}} \{F_{K^{\mathscr{M}}}(\{\widetilde{y}=0\}), F_{K^{\mathscr{M}}}(\{\widetilde{x}=0\}), F_{K^{\mathscr{M}}}(\{\widetilde{x}=\widetilde{y}\})\}.$$

   Let Γ_j, Γ_{j+1} be the two boundary arcs of Ω that meet at $\boldsymbol{A}_j$. Then there exists a line $e \in \ell$ such that the interior angles $\angle(e,\Gamma_j)$ and $\angle(e,\Gamma_{j+1})$ are both less than π.

REMARK 2.2 The last condition, requirement 8. in Definition 2.2, is merely a technical condition that results from our applying the regularity theory for singular perturbations of Melenk (2002). Very likely, it could be dropped.

The condition that $F_{K^{\mathscr{M}}}(\mathbf{0}) \in \partial\Omega$ or that $F_{K^{\mathscr{M}}}(\{\widetilde{y}=0\}) \subset \partial\Omega$ are not conditions on the patch geometry but on the maps $F_{K^{\mathscr{M}}}$. They are not essential but introduced for notational simplicity. They could be enforced by suitably concatenating the maps $F_{\mathscr{K}^{\mathscr{M}}}$ with an orthogonal transformation. ∎

REMARK 2.3 The meshes $\mathscr{T}^{L,n}_{geo,\sigma}$ are refined towards both vertices and edges of Ω. The parameter $L \in \mathbb{N}_0$ measures the number of layers of geometric refinement towards $\partial\Omega$ whereas the parameter $n \in \mathbb{N}$ characterizes the number of layers of geometric refinement towards the vertices. For $L = 0$ (or, more generally, L fixed), the meshes $\mathscr{T}^{0,n}_{geo,\sigma}$, $n = 1,2,\ldots$, realize the "geometric meshes" introduced in Babuška & Guo (1986a,b) (see also (Schwab, 1998, Sec. 4.4.1)) for the *hp*-FEM applied to elliptic boundary value problems with piecewise analytic data. ∎

EXAMPLE 2.3 Fig. 4 (left and middle) shows an example of an L-shaped domain with macro triangulation and suitable refinement patterns. ∎

2.4 *Geometric boundary layer meshes in curvilinear polygons*

Geometric boundary layer meshes can be constructed in various ways. A first approach, which is in line with the illustration in Fig. 4, is to create one layer of quadrilateral elements that partition a tubular neighborhood $T_{\partial\Omega}$ of $\partial\Omega$. Each quadrilateral K should fall into one of the following 3 categories: a) $\overline{K} \cap \partial\Omega$ is an edge of K; b) $\overline{K} \cap \partial\Omega$ consists of two contiguous edges and the shared vertex is a vertex of Ω; c) $\overline{K} \cap \partial\Omega$ is a vertex of Ω. In the second step, refinement patterns from Definition 2.2 are applied to each quadrilateral. In the final step, $\Omega' := \Omega \setminus T_{\partial\Omega}$ is triangulated under the constraint that the boundary nodes of the triangulation of Ω' on $\partial\Omega'$ coincide with the nodes of the triangulation of $T_{\partial\Omega}$ that also lie on $\partial\Omega'$. This triangulation of Ω' could be chosen to consist of triangles (and/or quadrilaterals). All elements of that triangulation will be denoted "trivial patches"; we mention without proof that the approximation result holds also if we include "trivial" triangles in the list of refinement patterns.

Geometric boundary layer meshes can also be constructed for general (curvilinear) polygons Ω starting from any regular initial triangulation $\mathscr{T}^0$ of Ω. This triangulation $\mathscr{T}^0$ is assumed to consist of (curvilinear) triangles with analytic element maps and satisfying the "usual" conditions for triangulations as spelled out in (Melenk, 2002, Def. 2.4.1). Then, the geometric boundary layer mesh is generated in 3 steps (cf. Fig. 5):

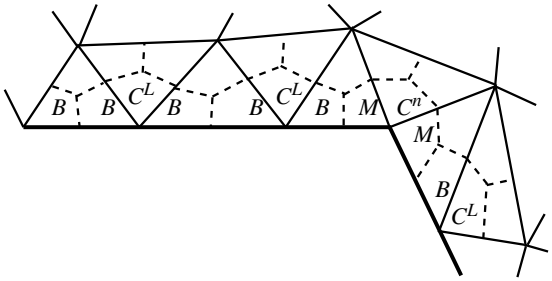

FIG. 5. Generating a boundary layer mesh from a regular triangulation $\mathscr{T}^0$: solid lines are the triangulation $\mathscr{T}^0$, dashed lines connect edge midpoints with element barycenters to create a mesh consisting of quadrilaterals. *B* stands for boundary layer patches $\widetilde{\mathscr{T}}^{\mathsf{BL},L}_{geo,\sigma}$, *M* for mixed patches $\widetilde{\mathscr{T}}^{\mathsf{M},L,n}_{geo,\sigma}$, C^L for corner layer patches $\widetilde{\mathscr{T}}^{\mathsf{C},L}_{geo,\sigma}$, C^n for corner layer patches $\widetilde{\mathscr{T}}^{\mathsf{C},n}_{geo,\sigma}$, empty quadrilaterals are trivial patches.

1. (Ensure condition 8 of Def. 2.2) For each vertex $\boldsymbol{A}_j$ of Ω verify if an edge e of $\mathscr{T}^0$ splits the interior angle at $\boldsymbol{A}_j$ into two angles each less than π. If not, then suitably split an appropriate triangle abuting on $\boldsymbol{A}_j$ into two triangles (so that the newly introduced edge will satisfy this condition) and remove the newly introduced hanging node by a mesh closure. The resulting triangulation has again analytic element maps and satisfies (Melenk, 2002, Def. 2.4.1); it is again denoted $\mathscr{T}^0$.

2. (Create a macro triangulation $\mathscr{T}^{\mathscr{M}}$ consisting of quadrilaterals only.) Split each triangle $K \in \mathscr{T}^0$ into 3 quadrilaterals as follows: split the reference triangle $\widehat{T}$ into 3 quadrilaterals $\widehat{K}_i$, $i = 1,2,3$, characterized by the vertices of $\widehat{T}$, its barycenter, and by the 3 midpoints of the edges of $\widehat{T}$. The element maps of the 3 quadrilaterals $F_K(\widehat{K}_i)$, $i = 1,2,3$, are obtained by concatenating the bilinear bijections $F_{\widehat{K}_i} : \widetilde{S} \to \widehat{K}_i$ with F_K. The triangulation $\mathscr{T}^{\mathscr{M}}$ of Ω obtained in this way realizes a decomposition of Ω into (curvilinear) quadrilaterals, and the element maps satisfy (Melenk, 2002, Def. 2.4.1).

3. (Generate the geometric boundary layer mesh.) The refinement pattern for each $K \in \mathscr{T}^{\mathscr{M}}$ is determined since K falls into exactly one of the categories 3—7 of Definition 2.2 as can be seen by the following observations: a) At most 2 edges of K are on $\partial\Omega$ (since the two edges that meet in the barycenter of the parent triangle cannot be on $\partial\Omega$). b) If two edges of K are situated on $\partial\Omega$, then they have to be subsets of the two edges of the parent triangle with common vertex $\boldsymbol{V}$; since $\mathscr{T}^0$ is a regular triangulation, the common vertex $\boldsymbol{V}$ has to be a vertex of Ω. Additionally, if necessary, the assumptions on where the reference element vertex $\mathbf{0}$ and/or the edges $\{\widetilde{y} = 0\}$, $\{\widetilde{x} = 0\}$ are mapped can be ensured by suitably adjusting the element map with the aid of an orthogonal transformation of $\widetilde{S}$. Finally, condition 8 of Def. 2.2 is satisfied by step 1.

It remains to see that after selecting the refinement patterns the resulting triangulation satisfies (Melenk, 2002, Def. 2.4.1). This follows from the fact that the parameters σ, L, n are the same for all macro elements and the structure of the refinement patterns: If an edge e of the macro triangulation inherits a further refinement from a refinement pattern, then the edge either lies on $\partial\Omega$ (which is immaterial for the question of satisfying (Melenk, 2002, Def. 2.4.1)) or it is in Ω and exactly one of its endpoints $\boldsymbol{V}$ lies on $\partial\Omega$. This edge e is shared by two macro elements. If $\boldsymbol{V}$ is a vertex of Ω, then the refinement patterns are such that the induced 1D-mesh on e is the same geometric mesh with n layers for both macro elements. If $\boldsymbol{V} \in \partial\Omega$ is not a vertex of Ω, then the induced 1D-mesh on e is the same geometric mesh with L layers for both macro elements. Hence, the resulting mesh satisfies (Melenk, 2002, Def. 2.4.1).

2.5 *Properties of the mesh patches*

We note that parts of the mixed patch, the tensor patch, and the corner patch are identical or at least structurally similar. For the analysis of the approximation properties of *hp*-FEM on geometric boundary layer meshes it is therefore convenient to single out these meshes:

DEFINITION 2.4 (half-patches, cf. Fig. 3) The *mixed half-patch* $\widetilde{\mathscr{T}}^{\mathsf{M},\mathrm{half},L,n}_{geo,\sigma}$ and the *corner half-patch* $\widetilde{\mathscr{T}}^{\mathsf{C},\mathrm{half},n}_{geo,\sigma}$ on $\widetilde{T}=\{(\widetilde{x},\widetilde{y})\,|\,0<\widetilde{x}<1,0<\widetilde{y}<\widetilde{x}\}$ are obtained by restricting $\widetilde{\mathscr{T}}^{\mathsf{M},L,n}_{geo,\sigma}$ and $\widetilde{\mathscr{T}}^{\mathsf{C},n}_{geo,\sigma}$ to $\widetilde{T}$. The *flipped corner half-patch* $\widetilde{\mathscr{T}}^{\mathsf{C},\mathrm{half},\mathrm{flip},n}_{geo,\sigma}$ on $T^{\mathrm{flip}}:=\{(\widetilde{x},\widetilde{y})\,|\,0<\widetilde{x}<1,\widetilde{x}<\widetilde{y}<1\}$ is obtained by reflecting $\widetilde{\mathscr{T}}^{\mathsf{C},\mathrm{half},n}_{geo,\sigma}$ at the diagonal $\{(\widetilde{x},\widetilde{x})\,|\,\widetilde{x}\in(0,1)\}$ of $\widetilde{S}$.

We will approximate functions on boundary layer meshes $\mathscr{T}^{L,n}_{geo,\sigma}$ with the aid of an elementwise defined operator Π_q. To estimate the total error in L^2-based norms, the elemental error contributions are summed up on each mesh patch separately. The following Lemma 2.1 provides tools to conveniently do that. In order to formulate Lemma 2.1, we introduce some additional notation, which represents the pull-back of the parts of the boundary of the reference patch that is mapped to $\partial\Omega$ and is marked by bold lines or dots in Figs. 2 and 3:

$$\Gamma^{C}:=\Gamma^{\mathsf{C},\mathrm{half}}:=\Gamma^{\mathsf{C},\mathrm{half},\mathrm{flip}}:=\{\mathbf{0}\}, \tag{2.1a}$$

$$\Gamma^{\mathsf{BL}}:=\Gamma^{\mathsf{M}}:=\Gamma^{\mathsf{M},\mathrm{half}}:=\{\widetilde{y}=0\}, \tag{2.1b}$$

$$\Gamma^{\mathsf{T}}:=\{\widetilde{y}=0\}\cup\{\widetilde{x}=0\}\cup\{\mathbf{0}\}. \tag{2.1c}$$

LEMMA 2.1 (properties of mesh patches) The reference patches (cf. Def. 2.1) and half patches (cf. Def. 2.4) have the following properties:

(i) The triangular elements $\widetilde{K}$ of the reference patches are shape regular with shape regularity constant depending solely on σ. For the rectangular elements $\widetilde{K}$ of the reference patches, the element maps $A_{\widetilde{K}}:\widehat{K}\to\widetilde{K}$ are affine with

$$A'_{\widetilde{K}}=\begin{pmatrix} h_{\widetilde{K},\widetilde{x}} & \\ & h_{\widetilde{K},\widetilde{y}}\end{pmatrix},$$

where $h_{\widetilde{K},\widetilde{x}}$, $h_{\widetilde{K},\widetilde{y}}\leqslant 1$ are the side lengths (in $\widetilde{y}$ and $\widetilde{x}$-direction) of $\widetilde{K}$. We denote

$$h_{\widetilde{K},min}:=\min\{h_{\widetilde{K},\widetilde{x}},h_{\widetilde{K},\widetilde{y}}\},\qquad h_{\widetilde{K},max}:=\max\{h_{\widetilde{K},\widetilde{x}},h_{\widetilde{K},\widetilde{y}}\}. \tag{2.2}$$

(ii) There is $c_{\mathrm{dist}}>0$ depending only on σ such that for all triangular elements $\widetilde{K}$ of a reference patch $\widetilde{\mathscr{T}}$ or a half-patch $\widetilde{\mathscr{T}}$ the following dichotomy holds: with $h_{\widetilde{K}}=\mathrm{diam}(\widetilde{K})$,

$$\text{either } \overline{\widetilde{K}}\cap\Gamma\neq\emptyset \quad\text{ or }\quad \mathrm{dist}(\widetilde{K},\Gamma)\geqslant c_{\mathrm{dist}}h_{\widetilde{K}},$$

and

$$\Gamma\in\{\Gamma^{\mathsf{C}},\Gamma^{\mathsf{C},\mathrm{half}},\Gamma^{\mathsf{C},\mathrm{half},\mathrm{flip}},\Gamma^{\mathsf{T}},\Gamma^{\mathsf{M}},\Gamma^{\mathsf{M},\mathrm{half}},\Gamma^{\mathsf{BL}}\}$$

for

$$\widetilde{\mathscr{T}}\in\{\widetilde{\mathscr{T}}^{\mathsf{C},n}_{geo,\sigma},\widetilde{\mathscr{T}}^{\mathsf{C},\mathrm{half},n}_{geo,\sigma},\widetilde{\mathscr{T}}^{\mathsf{C},\mathrm{half},\mathrm{flip},n}_{geo,\sigma},\widetilde{\mathscr{T}}^{\mathsf{T},n}_{geo,\sigma},\widetilde{\mathscr{T}}^{\mathsf{M},L,n}_{geo,\sigma},\widetilde{\mathscr{T}}^{\mathsf{M},\mathrm{half},L,n}_{geo,\sigma},\widetilde{\mathscr{T}}^{\mathsf{BL},L}_{geo,\sigma}\},$$

respectively.

(iii) There is $c_{\mathrm{dist}} > 0$ depending only on σ such that for all rectangular elements $\widetilde{K}$ of a reference patch $\widetilde{\mathscr{T}}$ or half-patch $\widetilde{\mathscr{T}}$, the following dichotomy holds:

$$\text{Either } \overline{\widetilde{K}} \cap \Gamma = \emptyset \quad \text{or} \quad \operatorname{dist}(\widetilde{K}, \Gamma) \geqslant c_{\mathrm{dist}} h_{\widetilde{K},min},$$

where

$$\Gamma \in \{\Gamma^{\mathsf{T}}, \Gamma^{\mathsf{M}}, \Gamma^{\mathsf{M,half}}, \Gamma^{\mathsf{BL}}\}$$

for

$$\widetilde{\mathscr{T}} \in \{\widetilde{\mathscr{T}}^{\mathsf{T},n}_{geo,\sigma}, \widetilde{\mathscr{T}}^{\mathsf{M},L,n}_{geo,\sigma}, \widetilde{\mathscr{T}}^{\mathsf{M,half},L,n}_{geo,\sigma}, \widetilde{\mathscr{T}}^{\mathsf{BL},L}_{geo,\sigma}\},$$

respectively.

(iv) There is $c_{\mathrm{dist}} > 0$ depending only on σ such that for all rectangular elements $\widetilde{K}$ of a mixed patch, a mixed half-patch, or a tensor patch there holds $\operatorname{dist}(\widetilde{K}, \mathbf{0}) \geqslant c_{\mathrm{dist}} h_{\widetilde{K},max}$.

(v) There is $C > 0$ depending only on σ such that for all elements $\widetilde{K}$ of a reference patch or half-patch there holds $\operatorname{dist}(\widetilde{K}, \mathbf{0}) \leqslant C \operatorname{diam} \widetilde{K}$.

(vi) Let $\delta > 0$ and consider a reference patch or half-patch. Let $\widetilde{\mathscr{T}}^{\triangle}$ be the collection of triangles of that reference patch or half-patch that do not abut on the vertex $\mathbf{0}$. Then, there exists a constant $C > 0$ depending solely on δ and σ such that

$$\sum_{\widetilde{K} \in \widetilde{\mathscr{T}}^{\triangle}} h_{\widetilde{K}}^{\delta} \leqslant C.$$

(vii) Let $\delta > 0$ and consider a reference mixed patch, tensor patch, mixed half-patch or corner half-patch. Let $\widetilde{\mathscr{T}}^{\square}$ be the collection of rectangles of that reference patch. Then there exists a constant $C > 0$ depending solely on δ and the parameter σ such that

$$\sum_{\widetilde{K} \in \widetilde{\mathscr{T}}^{\square}} \frac{h_{\widetilde{K},min}}{h_{\widetilde{K},max}} h_{\widetilde{K},max}^{\delta} \leqslant C.$$

(viii) Let $\delta \in (0,1]$, $\alpha > 0$, and consider a reference patch or half-patch. Let $\widetilde{\mathscr{T}}^{\triangle}$ be the collection of triangles of that reference patch or half-patch that do not abut on the vertex $\mathbf{0}$. Then, there holds, with a $C > 0$ depending solely on δ, α, and σ,

$$\forall \varepsilon \in (0,1]: \qquad \sum_{\widetilde{K} \in \widetilde{\mathscr{T}}^{\triangle}} (h_{\widetilde{K}}/\varepsilon)^{\delta} e^{-\alpha h_{\widetilde{K}}/\varepsilon} \leqslant C.$$

(ix) Let $\delta \in (0,1]$, $\alpha > 0$, and consider a reference mixed patch, mixed half-patch, or a reference tensor patch. Let $\widetilde{\mathscr{T}}^{\square}$ be the collection of rectangles of that reference patch. Then there exists a constant $C > 0$ depending solely on δ, α, and σ such that

$$\forall \varepsilon \in (0,1]: \qquad \sum_{\widetilde{K} \in \widetilde{\mathscr{T}}^{\square}} \frac{h_{\widetilde{K},min}}{h_{\widetilde{K},max}} (h_{\widetilde{K},max}/\varepsilon)^{\delta} e^{-\alpha h_{\widetilde{K},max}/\varepsilon} \leqslant C.$$

Proof. Items (i)–(v) follow by construction.

Since items (vi), (vii) are shown by similar arguments, we only prove the case of (vii) for the specific case of the mixed patch as shown in Fig. 2, bottom right panel. Inspection of that panel shows that for each $\widetilde{K} \in \widetilde{\mathscr{T}}^{\square}$ we have $h_{\widetilde{K},min} = h_{\widetilde{K},\widetilde{y}}$ and $h_{\widetilde{K},max} = h_{\widetilde{K},\widetilde{x}}$. Additionally, the elements can be enumerated as $K_{i,j}$, $i = 1,\dots,L$, $j = 1,\dots,i$ with $h_{K_{i,j},x} \sim \sigma^{L-i}$, $h_{K_{i,j},y} \sim \sigma^{L-j}$. Hence,

$$\sum_{\widetilde{K}\in\widetilde{\mathscr{T}}^{\square}} \frac{h_{\widetilde{K},min}}{h_{\widetilde{K},max}} h_{\widetilde{K},max}^{\delta} \lesssim \sum_{i=1}^{L}\sum_{j=1}^{i} \frac{\sigma^{L-j}}{\sigma^{L-i}} \sigma^{(L-i)\delta} \lesssim \sum_{i=1}^{L} \sigma^{\delta(L-i)} \lesssim 1. \tag{2.3}$$

The proof of items (viii), (ix) is also done in similar ways. Therefore, we will only show (ix). The key observation is that by comparing sums with integrals, there is a constant $C > 0$ depending solely on δ, α, and σ such that

$$\forall \varepsilon \in (0,1]: \quad \sum_{i=0}^{\infty} (\sigma^i/\varepsilon)^{\delta} e^{-\alpha\sigma^i/\varepsilon} \leqslant C. \tag{2.4}$$

The proof of (ix) now follows by a reasoning similar to that in (2.3). □

3. Approximation on the reference elements and on the reference configurations

In Sec. 3.1 we construct polynomial approximation operators on the reference square and triangle that coincide with the Gauss-Lobatto interpolant on the edges, which affords convenient H^1-conforming approximations. Sec. 3.2 studies the approximation properties of spaces of piecewise polynomials on the reference patches. It is shown that functions of boundary layer or corner layer type can be approximated at exponential rates, robustly in the parameter ε that characterizes the strength of the layer.

3.1 *Polynomial approximation operators on the reference element*

We introduce polynomial approximation operators on the reference triangle $\widehat{T}$ in Lemma 3.1 and the reference square $\widehat{S}$ in Lemma 3.2. Before actually doing so, we highlight a technical detail: the triangular elements (on the reference patches) are shape-regular so that isotropic scaling arguments can be brought to bear; only the rectangles (of the reference patches) may be anisotropic, for which tensor product polynomial approximation operators (specifically, the Gauss-Lobatto interpolation operator) are used for their favorable anisotropic scaling properties.

LEMMA 3.1 (element-by-element approximation on triangles) Let $\widehat{T}$ be the reference triangle. Then for every $q \in \mathbb{N}$, there exists a linear operator $\widehat{\Pi}_q^{\triangle} : C^0(\overline{\widehat{T}}) \to \mathbb{P}_q$ with the following properties:

(i) For each edge e of $\widehat{T}$, $(\widehat{\Pi}_q^{\triangle} u)|_e$ coincides with the Gauss-Lobatto interpolant $i_q(u|_e)$ of degree q on edge e.

(ii) (projection property) $\widehat{\Pi}_q^{\triangle} v = v$ for all $v \in \mathbb{P}_q$.

(iii) (stability) There exists a constant $C > 0$ such that for every $q \in \mathbb{N}$ there holds

$$\forall u \in W^{1,\infty}(\widehat{T}): \qquad \|u - \widehat{\Pi}_q^{\triangle} u\|_{W^{1,\infty}(\widehat{T})} \leqslant C q^4 \|\nabla u\|_{L^\infty(\widehat{T})},$$
$$\forall u \in C^0(\overline{\widehat{T}}): \qquad \|u - \widehat{\Pi}_q^{\triangle} u\|_{L^\infty(\widehat{T})} \leqslant C q^2 \|u\|_{L^\infty(\widehat{T})}.$$

(iv) Let $\boldsymbol{A}$ be one of the vertices of $\widehat{T}$ and $\beta \in [0,1)$. Then there is $C > 0$ (depending only on β) such that, provided the right-hand side is finite,

$$\|u - \widehat{\Pi}_q^{\triangle} u\|_{L^\infty(\widehat{T})} + \|u - \widehat{\Pi}_q^{\triangle} u\|_{H^1(\widehat{T})} \leqslant C q^4 \| \operatorname{dist}(\cdot, \boldsymbol{A})^\beta \nabla^2 u\|_{L^2(\widehat{T})}.$$

(v) Let $u \in C^\infty(\widehat{T})$ satisfy, for some C_u, $\gamma > 0$ and for some h, $\varepsilon \in (0,1]$,

$$\forall n \in \mathbb{N}_0 : \quad \|\nabla^n u\|_{L^\infty(\widehat{T})} \leqslant C_u \gamma^n h^n \max\{n+1, \varepsilon^{-1}\}^n.$$

Then there are δ, C, C', η, $b > 0$ depending solely on γ such that, under the provision that the *scale resolution condition*

$$\frac{h}{q\varepsilon} \leqslant \delta \tag{3.1}$$

is satisfied, there holds

$$\|u - \widehat{\Pi}_q^{\triangle} u\|_{W^{1,\infty}(\widehat{T})} \leqslant C' C_u \left(\left(\frac{h}{h+\eta} \right)^{q+1} + \left(\frac{h}{q\varepsilon\eta} \right)^{q+1} \right) \leqslant C C_u e^{-bq} \min\{1, h/\varepsilon\}.$$

Proof. The operator $\widehat{\Pi}_q^{\triangle}$ is taken as the one defined in (Melenk, 2002, Thm. 3.2.20), where items (i)–(iii) are shown (the $W^{1,\infty}$-estimate follows with an additional polynomial inverse estimate). Item (iv) is taken from (Melenk, 2002, Prop. 3.2.21). For Item (v), we note that the projection property of (ii) and the stability assertions (iii) reduce the error estimate to a best approximation problem, which can be taken from (Melenk & Sauter, 2010, Lemma C.2). □

LEMMA 3.2 (approximation properties of the Gauss-Lobatto interpolant) Let $\widehat{S}$ be the reference square. For each $q \in \mathbb{N}$ the tensor-product Gauss-Lobatto interpolation operator $\widehat{\Pi}_q^{\square} : C^0(\overline{\widehat{S}}) \to \mathbb{Q}_q$ satisfies the following:

(i) (projection property) $\widehat{\Pi}_q^{\square} v = v$ for all $v \in \mathbb{Q}_q$.

(ii) For each edge e, the restriction $(\widehat{\Pi}_q^{\square} u)|_e$ coincides with the univariate Gauss-Lobatto interpolant $i_q(u|_e)$ on e.

(iii) (stability)

$$\begin{aligned}
&\forall u \in C^0(\overline{\widehat{S}}): && \|u - \widehat{\Pi}_q^{\square} u\|_{L^\infty(\widehat{S})} \leqslant C q \|u\|_{L^\infty(\widehat{S})}, \\
&\forall u \in C^1(\overline{\widehat{S}}): && \|\partial_{\hat{x}}(u - \widehat{\Pi}_q^{\square} u)\|_{L^\infty(\widehat{S})} \leqslant C q^4 \|\partial_x u\|_{L^\infty(\widehat{S})}, \\
&\forall u \in C^1(\overline{\widehat{S}}): && \|\partial_{\hat{y}}(u - \widehat{\Pi}_q^{\square} u)\|_{L^\infty(\widehat{S})} \leqslant C q^4 \|\partial_y u\|_{L^\infty(\widehat{S})}.
\end{aligned}$$

(iv) Let $u \in C^\infty(\widehat{S})$ satisfy for some C_u, $\gamma > 0$, ε_x, ε_y, h_x, $h_y \in (0,1]$ and all $(n,m) \in \mathbb{N}_0^2$

$$\|\partial_{\hat{x}}^m \partial_{\hat{y}}^n u\|_{L^\infty(\widehat{S})} \leqslant C_u \gamma^{n+m} h_x^m h_y^n \max\{n+1, \varepsilon_y^{-1}\}^n \max\{m+1, \varepsilon_x^{-1}\}^m. \tag{3.2}$$

Then there are constants δ, C, η, $b > 0$ depending solely on γ such that under the scale-resolution condition

$$\frac{h_x}{q\varepsilon_x} + \frac{h_y}{q\varepsilon_y} \leqslant \delta \tag{3.3}$$

there holds

$$
\begin{aligned}
&\|\partial_{\widehat{x}}(u-\widehat{\Pi}_q^{\square}u)\|_{L^\infty(\widehat{S})}\\
&\leqslant CC_u\frac{h_x}{\varepsilon_x}\left[\varepsilon_x\left(\frac{h_x}{h_x+\eta}\right)^q+\left(\frac{h_x}{\varepsilon_x q\eta}\right)^q+\left(\frac{h_y}{h_y+\eta}\right)^{q+1}+\left(\frac{h_y}{\varepsilon_y q\eta}\right)^{q+1}\right],\\
&\|\partial_{\widehat{y}}(u-\widehat{\Pi}_q^{\square}u)\|_{L^\infty(\widehat{S})}\\
&\leqslant CC_u\frac{h_y}{\varepsilon_y}\left[\left(\frac{h_x}{h_x+\eta}\right)^{q+1}+\left(\frac{h_x}{\varepsilon_x q\eta}\right)^{q+1}+\varepsilon_y\left(\frac{h_y}{h_y+\eta}\right)^q+\left(\frac{h_y}{\varepsilon_y q\eta}\right)^q\right],\\
&\|u-\widehat{\Pi}_q^{\square}u\|_{L^\infty(\widehat{S})}\\
&\leqslant CC_u\left[\left(\frac{h_x}{h_x+\eta}\right)^{q+1}+\left(\frac{h_x}{\varepsilon_x q\eta}\right)^{q+1}+\left(\frac{h_y}{h_y+\eta}\right)^{q+1}+\left(\frac{h_y}{\varepsilon_y q\eta}\right)^{q+1}\right].
\end{aligned}
$$

Proof. Items (i), (ii) are well-known. We let Λ_q denote the Lebesgue constant of the univariate Gauss-Lobatto interpolation operator of polynomial degree $q\in\mathbb{N}$ (cf. Lemma A.2). The L^∞-stability in (iii) follows from tensor product arguments, viz. $\|\widehat{\Pi}_q^{\square}u\|_{L^\infty(\widehat{S})}\leqslant\Lambda_q^2\|u\|_{L^\infty(\widehat{S})}$ and the (generous) bound $\Lambda_q^2\leqslant Cq$ for $q\geqslant 1$. For the remaining estimates, we introduce the tensor-product Gauss-Lobatto interpolation operator $\widehat{\Pi}_q^{\square}=i_q\otimes i_q=i_q^{\widehat{x}}\otimes i_q^{\widehat{y}}$, where we use the superscipts $\widehat{x}$ and $\widehat{y}$ to emphasize the variable with respect to which the univariate Gauss-Lobatto interpolant acts. From

$$
u-i_q^{\widehat{y}}\otimes i_q^{\widehat{x}}u=u-(\mathrm{I}\otimes i_q^{\widehat{y}})u+\mathrm{I}\otimes i_q^{\widehat{y}}(u-i_q^{\widehat{x}}\otimes\mathrm{I}u)
$$

we get in view of the univariate stability bound Lemma A.2

$$
\begin{aligned}
\|\partial_{\widehat{x}}(u-i_q^{\widehat{x}}\otimes i_p^{\widehat{y}}u)\|_{L^\infty(\widehat{S})}&\lesssim\Lambda_q\sup_{\widehat{x}\in(0,1)}\inf_{v\in\mathbb{P}_q}\|\partial_{\widehat{x}}u(x,\cdot)-v\|_{L^\infty(0,1)}\\
&\quad+q^2\Lambda_q^2\sup_{\widehat{y}\in(0,1)}\inf_{v\in\mathbb{P}_q}\|\partial_{\widehat{x}}(u(\cdot,\widehat{y})-v)\|_{L^\infty(0,1)};
\end{aligned}
\tag{3.4}
$$

an analogous estimate holds for $\partial_y(u-i_q^{\widehat{x}}\otimes i_q^{\widehat{y}}u)$. The estimate (3.4) gives the stability estimates in $W^{1,\infty}$ of (iii) by selecting $v=0$ in the infima. The estimate (3.4) reduces the question of approximation on $\widehat{S}$ to questions of univariate polynomial approximation. The pertinent approximation results to prove item (iv) are given in Lemma A.1. □

3.2 *Approximation on the reference patches*

In this section, we study the approximation of functions on the reference patches (or the half-patches) described in Defs. 2.1, 2.4. The non-trivial reference patches consist of meshes that are refined towards $\mathbf{0}$, which can resolve algebraic singularities at $\mathbf{0}$, and meshes that are anisotropically refined towards the edge $\{\widetilde{y}=0\}$, which can resolve algebraic singularities at $\{\widetilde{y}=0\}$ or boundary layers. We show exponential approximability of functions that have algebraic singularities at $\mathbf{0}$ or boundary layers at $\{\widetilde{y}=0\}$. Throughout this section, we will use the notation

$$
\widetilde{r}(\cdot):=\operatorname{dist}(\mathbf{0},\cdot).
\tag{3.5}
$$

In this section, we present piecewise polynomial approximations on reference patches using the following elementwise defined interpolation operator:

$$(\widetilde{\Pi}_q)|_{\widetilde{K}} u := \begin{cases} \widehat{\Pi}_q^{\triangle}(u \circ A_{\widetilde{K}}) & \text{if } \widetilde{K} \text{ is a triangle } \triangle \\ \widehat{\Pi}_q^{\square}(u \circ A_{\widetilde{K}}) & \text{if } \widetilde{K} \text{ is a rectangle } \square, \end{cases} \tag{3.6}$$

where $A_{\widetilde{K}} : \widehat{K} \to \widetilde{K} = A_{\widetilde{K}}(\widehat{K}) \subset \widetilde{S}$ is the affine bijection between the reference element and the corresponding element on the reference patch. The edge-traces of the interpolators $\widehat{\Pi}_q^{\triangle}$ and $\widehat{\Pi}_q^{\square}$ coincide with the univariate Gauss-Lobatto interpolation operator on the edges of $\widehat{K}$. Hence, H^1-conformity of the elementwise defined operator $\widetilde{\Pi}_q$ is ensured. We will frequently use the stability estimates

$$\|\widetilde{\Pi}_q u\|_{L^\infty(\widetilde{K})} \leqslant Cq^2 \|u\|_{L^\infty(\widetilde{K})}, \qquad \|\nabla \widetilde{\Pi}_q u\|_{L^\infty(\widetilde{K})} \leqslant Cq^4 \|\nabla u\|_{L^\infty(\widetilde{K})}; \tag{3.7}$$

these estimates are easily seen to hold for triangles with the isotropic scaling property and Lemma 3.1, (iii). The anisotropic nature of the rectangles is accounted for by separately scaling the bounds for the partial derivatives in Lemma 3.2, (iii).

3.2.1 *hp-FE approximation of corner singularity functions.*

LEMMA 3.3 (approximation of corner singularity functions)

(i) Let $\widetilde{\mathscr{T}} \in \{\widetilde{\mathscr{T}}^{\mathsf{M},\mathrm{half},L,n}_{geo,\sigma}, \widetilde{\mathscr{T}}^{\mathsf{C},\mathrm{half},n}_{geo,\sigma}, \widetilde{\mathscr{T}}^{\mathsf{C},\mathrm{half},\mathrm{flip},n}_{geo,\sigma}, \widetilde{\mathscr{T}}^{\mathsf{C},n}_{geo,\sigma}, \widetilde{\mathscr{T}}^{\mathsf{T},n}_{geo,\sigma}\}$. Let $\mathscr{O}$ be the region covered by the elements of $\widetilde{\mathscr{T}}$, i.e., let $\mathscr{O} = \widetilde{S}$ if $\widetilde{\mathscr{T}} \in \{\widetilde{\mathscr{T}}^{\mathsf{C},n}_{geo,\sigma}, \widetilde{\mathscr{T}}^{\mathsf{T},n}_{geo,\sigma}\}$ is a full reference patch, $\mathscr{O} = \widetilde{T}$ if $\widetilde{\mathscr{T}} \in \{\widetilde{\mathscr{T}}^{\mathsf{C},\mathrm{half},n}_{geo,\sigma}, \widetilde{\mathscr{T}}^{\mathsf{M},\mathrm{half},L,n}_{geo,\sigma}\}$ is a reference half-patch, and $\mathscr{O} = T^{\mathrm{flip}}$ if $\widetilde{\mathscr{T}} = \widetilde{\mathscr{T}}^{\mathsf{C},\mathrm{half},\mathrm{flip},n}_{geo,\sigma}$. Let $\widetilde{u}$ be analytic on $\overline{\mathscr{O}}$ and assume there exist constants $\varepsilon \in (0,1]$, $\beta \in [0,1)$, γ, $C_u > 0$ such that for all $p \in \mathbb{N}_0$ and all $\widetilde{\mathbf{x}} \in \widetilde{S}$

$$|\nabla^p(\widetilde{u}(\widetilde{\mathbf{x}}) - \widetilde{u}(\mathbf{0}))| \leqslant C_u \varepsilon^{-1} \gamma^p (\widetilde{r}(\widetilde{\mathbf{x}})/\varepsilon)^{1-\beta} \widetilde{r}(\widetilde{\mathbf{x}})^{-p} \max\{p+1, \widetilde{r}(\widetilde{\mathbf{x}})/\varepsilon\}^{p+1}. \tag{3.8}$$

Then, there are constants C, b, $\kappa > 0$ depending only on γ, σ, and β (in particular, independent of ε, n, L) such that under the scale resolution condition

$$q\varepsilon \geqslant \kappa \tag{3.9}$$

there holds

$$\|\widetilde{u} - \widetilde{\Pi}_q \widetilde{u}\|_{L^\infty(\mathscr{O})} + \|\nabla(\widetilde{u} - \widetilde{\Pi}_q \widetilde{u})\|_{L^2(\mathscr{O})} \leqslant CC_u \left(q^9 \sigma^{n(1-\beta)} + e^{-bq}\right). \tag{3.10}$$

(ii) Let $\widetilde{\mathscr{T}} \in \{\widetilde{\mathscr{T}}^{\mathsf{BL},L}, \widetilde{S}\}$. Let $\widetilde{u}$ be analytic on $\widetilde{S}$ and assume that there are constants C_u, $\gamma > 0$ such that for all $p \in \mathbb{N}_0$

$$\|\nabla^p \widetilde{u}\|_{L^\infty(\widetilde{S})} \leqslant C_u \gamma^p \max\{p+1, \varepsilon^{-1}\}^{p+1}. \tag{3.11}$$

Then there are constants C, b, $\kappa > 0$ depending only on γ and σ (in particular, they are independent of ε and L) such that under the constraint (3.9) there holds

$$\|\widetilde{u} - \widetilde{\Pi}_q \widetilde{u}\|_{W^{1,\infty}(\widetilde{S})} \leqslant CC_u e^{-bq}. \tag{3.12}$$

Proof. Proof of (i): Step 1: Elements abutting on $\mathbf{0}$*:* Only triangles $\triangle$ may abut on $\mathbf{0}$. Let $\widetilde{K}$ be such a triangle. From (3.8) and estimating (generously) $\max\{1,\widetilde{r}(\cdot)/\varepsilon\}^3 \lesssim \varepsilon^{-3}$, we get the existence of $C>0$ independent of $\varepsilon\in(0,1]$ with

$$\forall \widetilde{\mathbf{x}}\in\widetilde{K}: \quad |\nabla^2\widetilde{u}(\widetilde{\mathbf{x}})| \leqslant C(\widetilde{r}(\widetilde{\mathbf{x}}))^{-1-\beta}\varepsilon^{-5+\beta}. \tag{3.13}$$

By scaling this bound and invoking Lemma 3.1, (iv), we get with $h_{\widetilde{K}} := \operatorname{diam}\widetilde{K}$ for any fixed $\widetilde{\beta}\in(\beta,1)$

$$\begin{aligned}\|\widetilde{u}-\widetilde{\Pi}_q\widetilde{u}\|_{L^\infty(\widetilde{K})} + \|\nabla(\widetilde{u}-\widetilde{\Pi}_q\widetilde{u})\|_{L^2(\widetilde{K})} &\leqslant Cq^4 h_{\widetilde{K}}^{1-\widetilde{\beta}}\|\widetilde{r}^{\widetilde{\beta}}\nabla^2\widetilde{u}\|_{L^2(\widetilde{K})} \\ &\overset{(3.13)}{\leqslant} Cq^4 h_{\widetilde{K}}^{1-\widetilde{\beta}}\varepsilon^{-5+\beta}h_{\widetilde{K}}^{\widetilde{\beta}-\beta} \overset{q\varepsilon\geqslant\kappa}{\leqslant} Cq^{4+5-\beta}h_{\widetilde{K}}^{1-\beta} \lesssim q^{9-\beta}\sigma^{n(1-\beta)}.\end{aligned} \tag{3.14}$$

Step 2: Elements not abutting on $\mathbf{0}$*:* From Lemma 2.1, (v) we get $\widetilde{r}(\cdot)\lesssim h_{\widetilde{K}} = \operatorname{diam}\widetilde{K}$ on $\widetilde{K}$. The regularity assumption (3.8) then implies that there exist (suitably adjusted) constants C, γ such that for all $p\in\mathbb{N}_0$

$$\|\nabla^p(\widetilde{u}-\widetilde{u}(\mathbf{0}))\|_{L^\infty(\widetilde{K})} \leqslant C\gamma^p\varepsilon^{-3+\beta}h_{\widetilde{K}}^{1-\beta}\widetilde{r}^{-p}\max\{p+1,\varepsilon^{-1}\}^p\,. \tag{3.15}$$

We now consider the approximation on triangles and rectangles separately.

Step 2.1: $\widetilde{K}$ *is a triangle* $\triangle$. Lemma 2.1, (ii) implies in particular that $h_{\widetilde{K}}\lesssim\widetilde{r}(\cdot)$ on $\widetilde{K}$. Scaling the bounds (3.15) to the reference element $\widehat{K}=\widehat{T}$ therefore gives for $\widehat{u}:=\widetilde{u}\circ A_{\widetilde{K}}$, where $A_{\widetilde{K}}:\widehat{K}\to\widetilde{K}$ is the affine element map for $\widetilde{K}$, the existence of constants C, $\gamma>0$ such that

$$\forall p\in\mathbb{N}_0: \quad \|\widehat{\nabla}^p(\widehat{u}-\widehat{u}(\mathbf{0}))\|_{L^\infty(\widehat{K})} \leqslant C\gamma^p\varepsilon^{-3+\beta}h_{\widetilde{K}}^{1-\beta}\max\{p+1,\varepsilon^{-1}\}^p\,. \tag{3.16}$$

In order to be able to apply the approximation properties of Lemma 3.1, we note

$$\begin{aligned}\max\{p+1,\varepsilon^{-1}\}^p &= \max\{(p+1)^p,\varepsilon^{-p}(p+1)^{-p}(p+1)^p\} \\ &= (p+1)^p\max\{1,\varepsilon^{-p}(p+1)^{-p}\} \leqslant (p+1)^p\max\left\{1,\frac{(1/\varepsilon)^p}{p!}\right\} \\ &\leqslant (p+1)^p e^{1/\varepsilon} \overset{q\varepsilon\geqslant\kappa}{\leqslant} (p+1)^p e^{q/\kappa}.\end{aligned} \tag{3.17}$$

Inserting (3.17) into (3.16) yields that there are constants $C>0$, $\gamma>0$ such that

$$\forall p\in\mathbb{N}_0: \quad \|\nabla^p(\widehat{u}-\widehat{u}(\mathbf{0}))\|_{L^\infty(\widehat{K})} \leqslant Ce^{q/\kappa}\varepsilon^{-3+\beta}h_{\widetilde{K}}^{1-\beta}\gamma^p(p+1)^p. \tag{3.18}$$

We are in a position to apply Lemma 3.1. The parameter δ in (3.1) is determined by γ. In view of $q\varepsilon\geqslant\kappa$, we can ensure condition (3.1) by selecting κ sufficiently large to obtain from Lemma 3.1 with some $b>0$ depending only on γ

$$\|\widehat{u}-\widehat{\Pi}_q^{\triangle}\widehat{u}\|_{W^{1,\infty}(\widehat{K})} \leqslant Ch_{\widetilde{K}}^{1-\beta}e^{q/\kappa}\varepsilon^{-3+\beta}e^{-bq}.$$

We may assume that κ is so large that $1/\kappa-b\leqslant -b/2$ to estimate $e^{q/\kappa}e^{-bq}\leqslant e^{-qb/2}$. Finally, in view of $q\varepsilon\geqslant\kappa$, we can also absorb the factor $\varepsilon^{-3+\beta}\lesssim q^{3-\beta}$ in the exponentially decaying one by adjusting b. Upon scaling from $\widehat{K}$ to $\widetilde{K}$ we get the existence of constants b, $C>0$ such that

$$\forall q\in\mathbb{N}: \quad \|\widetilde{u}-\widetilde{\Pi}_q\widetilde{u}\|_{L^\infty(\widetilde{K})} + \|\nabla(\widetilde{u}-\widetilde{\Pi}_q\widetilde{u})\|_{L^2(\widetilde{K})} \leqslant Ch_{\widetilde{K}}^{1-\beta}e^{-bq}. \tag{3.19}$$

Step 2.2: $\widetilde{K}$ is a rectangle $\square$. We argue as in the case of a triangle in Step 2.1. Starting point is again the regularity assertion (3.8). The rectangle $\widetilde{K}$ has side lengths $h_{\widetilde{K},\widetilde{y}} \leqslant h_{\widetilde{K},\widetilde{x}} \leqslant 1$. From Lemma 2.1, (iv) we have $h_{\widetilde{K},\widetilde{y}} \leqslant h_{\widetilde{K},\widetilde{x}} \leqslant C\widetilde{r}(\cdot)$ on $\widetilde{K}$. Hence, the (anisotropic) scaling to the reference square $\widehat{S}$ of the estimates (3.8) yields, for all $(n,m) \in \mathbb{N}_0^2$, in view of (3.17)

$$\begin{aligned}\|\partial_x^m \partial_y^n (\widehat{u} - \widehat{u}(\mathbf{0}))\|_{L^\infty(\widehat{S})} &\leqslant C\varepsilon^{-3+\beta} h_{\widetilde{K},\widetilde{x}}^{1-\beta} \gamma^{n+m} h_{\widetilde{K},x}^m h_{\widetilde{K},y}^n h_{\widetilde{K},\widetilde{x}}^{-(n+m)} e^{q/\kappa} (n+m)^{n+m} \\ &\overset{(A.9)}{\leqslant} \varepsilon^{-3+\beta} h_{\widetilde{K},\widetilde{x}}^{1-\beta} \gamma^{n+m} e^{q/\kappa} n!m!, \end{aligned} \tag{3.20}$$

where we again suitably adjusted the value of γ. Lemma 3.2 (with $h_y = h_{\widetilde{K},\widetilde{y}}/h_{\widetilde{K},\widetilde{x}} \leqslant 1$ and $\varepsilon_x = \varepsilon_y = 1$ there) yields with the regularity estimates (3.20) the existence of constants C, $b > 0$ such that for all $q \in \mathbb{N}_0$

$$\begin{aligned}\|\widehat{u} - \widehat{\Pi}_q^{\square} \widehat{u}\|_{L^\infty(\widehat{K})} + \|\partial_{\widehat{x}}(\widehat{u} - \widehat{\Pi}_q^{\square} \widehat{u})\|_{L^\infty(\widehat{K})} &\leqslant C\varepsilon^{-3+\beta} h_{\widetilde{K},\widetilde{x}}^{1-\beta} e^{-bq}, \\ \|\partial_{\widehat{y}}(\widehat{u} - \widehat{\Pi}_q^{\square} \widehat{u})\|_{L^\infty(\widehat{K})} &\leqslant C\varepsilon^{-3+\beta} h_{\widetilde{K},\widetilde{x}}^{1-\beta} \frac{h_{\widetilde{K},\widetilde{y}}}{h_{\widetilde{K},\widetilde{x}}} e^{-bq}, \end{aligned}$$

where the factor $e^{q/\kappa}$ was absorbed again in the exponentially decaying term by taking κ sufficiently large. We obtain on $\widetilde{S}$

$$\|\partial_{\widetilde{x}}(\widetilde{u} - \widetilde{\Pi}_q \widetilde{u})\|_{L^2(\widetilde{S})} \leqslant C\varepsilon^{-3+\beta} \sqrt{h_{\widetilde{K},\widetilde{x}} h_{\widetilde{K},\widetilde{y}}} h_{\widetilde{K},\widetilde{x}}^{-1} h_{\widetilde{K},\widetilde{x}}^{1-\beta} e^{-bq} \overset{q\varepsilon \geqslant \kappa}{\leqslant} C\sqrt{h_{\widetilde{K},\widetilde{y}}/h_{\widetilde{K},\widetilde{x}}} h_{\widetilde{K},\widetilde{x}}^{1-\beta} e^{-bq}, \tag{3.21a}$$

$$\|\partial_{\widetilde{y}}(\widetilde{u} - \widetilde{\Pi}_q \widetilde{u})\|_{L^2(\widetilde{S})} \leqslant C\sqrt{h_{\widetilde{K},\widetilde{y}}/h_{\widetilde{K},\widetilde{x}}} h_{\widetilde{K},\widetilde{x}}^{1-\beta} e^{-bq}, \tag{3.21b}$$

$$\|(\widetilde{u} - \widetilde{\Pi}_q \widetilde{u})\|_{L^\infty(\widetilde{S})} \leqslant C h_{\widetilde{K},\widetilde{x}}^{1-\beta} e^{-bq}, \tag{3.21c}$$

where again we adjusted the values of the constants b, C in the estimates to absorb algebraic factors in q.

Step 3: Summation of the elemental errors: We note that the element size $h_{\widetilde{K}}$ of the elements abutting on $\mathbf{0}$ is $h_{\widetilde{K}} \sim \sigma^n$. For the finitely many contributions from the (triangular) elements $\widetilde{K}$ touching $\mathbf{0}$ we have by (3.14) the existence of $C > 0$ such that for every $q \geqslant 1$

$$\sum_{\widetilde{K}:\, \mathbf{0} \in \overline{\widetilde{K}}} \|\widetilde{u} - \widetilde{\Pi}_q \widetilde{u}\|_{H^1(\widetilde{K})}^2 \overset{(3.14)}{\leqslant} C q^{18} \sigma^{2n(1-\beta)}.$$

The sum of squared error contributions over all triangular elements not touching $\mathbf{0}$ is also bounded by e^{-2bq} by combining (3.19) and Lemma 2.1, (vi). Likewise, the sum over all rectangular elements is bounded by e^{-2bq} by combining (3.21) and Lemma 2.1, (vii).

Proof of (ii): The proof is similar to the proof of case (i) and can be obtained from it by formally setting $\beta = 0$ and $\widetilde{r} \equiv 1$ and dropping the error contribution $q^9 \sigma^{n(1-\beta)}$ that is due to the small elements touching $\mathbf{0}$. $\square$

3.2.2 *hp-FE approximation of boundary layer functions.*

LEMMA 3.4 (approximation of boundary layer functions) Fix $c_1 > 0$.

(i) Let $\widetilde{\mathscr{T}} \in \{\widetilde{\mathscr{T}}^{\mathsf{M,half},L,n}_{geo,\sigma}, \widetilde{\mathscr{T}}^{\mathsf{BL},L}_{geo,\sigma}\}$. Let $\widetilde{\mathscr{T}'} \subset \widetilde{\mathscr{T}}$ and let $\mathscr{O} := \mathrm{interior}\big(\cup\{\overline{\widetilde{K}} \,|\, \widetilde{K} \in \widetilde{\mathscr{T}'}\}\big)$ be the union of the elements of $\widetilde{\mathscr{T}'}$. Let $\widetilde{u}$ be analytic on $\mathscr{O}$ and satisfy for some C_u, γ, $\alpha > 0$, $\varepsilon \in (0,1]$ and for all $(m,n) \in \mathbb{N}_0^2$ and all $\widetilde{\mathbf{x}} = (\widetilde{x},\widetilde{y}) \in \mathscr{O}$

$$|\partial_{\widetilde{x}}^m \partial_{\widetilde{y}}^n \widetilde{u}(\widetilde{\mathbf{x}})| \leqslant C_u \gamma^{n+m} m! \max\{n, \varepsilon^{-1}\}^n e^{-\alpha\widetilde{y}/\varepsilon}. \tag{3.22}$$

Assume that L is such that the *scale resolution condition*

$$\sigma^L \leqslant c_1 \varepsilon \tag{3.23}$$

is satisfied. Then there are constants C, $b > 0$ depending only on γ, α, c_1, σ such that

$$\forall q \in \mathbb{N}\colon \quad \|\widetilde{u} - \widetilde{\Pi}_q \widetilde{u}\|_{L^\infty(\mathscr{O})} + \varepsilon \|\nabla(\widetilde{u} - \widetilde{\Pi}_q \widetilde{u})\|_{L^\infty(\mathscr{O})} \leqslant C C_u e^{-bq}. \tag{3.24}$$

(ii) Let $\widetilde{\mathscr{T}''} \subset \widetilde{\mathscr{T}}^{\mathsf{C,half},n}_{geo,\sigma}$ or $\widetilde{\mathscr{T}''} \subset \widetilde{\mathscr{T}}^{\mathsf{C,half,flip},n}_{geo,\sigma}$. Let $\mathscr{O} := \mathrm{interior}\big(\cup\{\overline{\widetilde{K}} \,|\, \widetilde{K} \in \widetilde{\mathscr{T}''}\}\big)$ be the union of the elements of $\widetilde{\mathscr{T}''}$. Let $\widetilde{u}$ be analytic on $\mathscr{O}$ and satisfy for some C_u, γ, $\alpha > 0$, $\varepsilon \in (0,1]$

$$\forall p \in \mathbb{N}_0\ \forall \widetilde{\mathbf{x}} \in \mathscr{O}\colon \quad |\nabla^p \widetilde{u}(\widetilde{\mathbf{x}})| \leqslant C_u \gamma^p \max\{p, \varepsilon^{-1}\}^p e^{-\alpha\widetilde{r}(\widetilde{\mathbf{x}})/\varepsilon}. \tag{3.25}$$

Assume that n is such that $c_1 > 0$, $n \in \mathbb{N}$ satisfies the *scale scale resolution condition*

$$\sigma^n \leqslant c_1 \varepsilon \tag{3.26}$$

is satisfied. Then, there are constants C, $b > 0$ (depending only on γ, α, c_1, σ) such that

$$\forall q \in \mathbb{N}\colon \quad \|\widetilde{u} - \widetilde{\Pi}_q \widetilde{u}\|_{L^\infty(\mathscr{O})} + \varepsilon \|\nabla(\widetilde{u} - \widetilde{\Pi}_q \widetilde{u})\|_{L^\infty(\mathscr{O})} \leqslant C C_u e^{-bq}. \tag{3.27}$$

Proof. Proof of (ii): We only consider the case $\mathscr{T}'' \subset \widetilde{\mathscr{T}}^{\mathsf{C,half},n}_{geo,\sigma}$ as the case $\mathscr{T}'' \subset \widetilde{\mathscr{T}}^{\mathsf{C,half,flip},n}_{geo,\sigma}$ is handled similarly. We note that the patch $\widetilde{\mathscr{T}}^{\mathsf{C,half},n}_{geo,\sigma}$ consists of triangles only, which are all shape-regular. Let $\widetilde{K} \subset \mathscr{O}$ be a triangle and let $h_{\widetilde{K}} = \operatorname{diam}\widetilde{K}$. In the case that $\widetilde{K}$ touches $\mathbf{0}$, the condition (3.26) implies that $h_{\widetilde{K}} \lesssim \sigma^n \lesssim c_1\varepsilon$ so that

$$\frac{h_{\widetilde{K}}}{q\varepsilon} \lesssim \frac{1}{q}. \tag{3.28}$$

Hence, for every fixed choice of the constant c_1 there exists $q_0 = q_0(c_1) \in \mathbb{N}$ (independent of ε) such that for every $q \geqslant q_0$ one has the scale resolution condition (3.1). Then, Lemma 3.1, (v) implies for suitable $b > 0$ (independent of ε)

$$\|\widetilde{u} - \widetilde{\Pi}_q \widetilde{u}\|_{L^\infty(\widetilde{K})} + \varepsilon \|\nabla(\widetilde{u} - \widetilde{\Pi}_q \widetilde{u})\|_{L^\infty(\widetilde{K})} \lesssim e^{-bq}. \tag{3.29}$$

If $\widetilde{K}$ does not touch $\mathbf{0}$, we distinguish between two further cases. In the first case, we assume that $h_{\widetilde{K}}/(q\varepsilon) \leqslant \delta$ and proceed as above: The scale resolution condition (3.1) is satisfied, and we arrive again at (3.29). In the case $h_{\widetilde{K}}/(q\varepsilon) \geqslant \delta$, we note that Lemma 2.1, (ii) implies $\operatorname{dist}(\widetilde{K}, \mathbf{0}) \geqslant c_2 h_{\widetilde{K}} \geqslant c_2 \delta q \varepsilon$. Hence, by the decay properties of $\widetilde{u}$ in (3.25) we have

$$\|\widetilde{u}\|_{L^\infty(\widetilde{K})} + \varepsilon \|\nabla \widetilde{u}\|_{L^\infty(\widetilde{K})} \leqslant C e^{-\alpha c_2 h_{\widetilde{K}}/\varepsilon} \leqslant C e^{-\alpha c_2 q \delta}. \tag{3.30}$$

In view of the stability properties (3.7), we conclude

$$\|\widetilde{u}-\widetilde{\Pi}_q\widetilde{u}\|_{L^\infty(\widetilde{K})}+\varepsilon\|\nabla(\widetilde{u}-\widetilde{\Pi}_q\widetilde{u})\|_{L^\infty(\widetilde{K})}\lesssim e^{-bq}. \tag{3.31}$$

Proof of (i): We distinguish between triangular and rectangular elements.

Approximation of $\widetilde{u}$ on triangular elements $\widetilde{K}$: Triangular elements do not appear in boundary layer patches $\widetilde{\mathscr{T}}^{\mathsf{BL},L}_{geo,\sigma}$ but only in $\widetilde{\mathscr{T}}^{\mathsf{M},\mathrm{half},L,n}_{geo,\sigma}$. For patches $\widetilde{\mathscr{T}}^{\mathsf{M},\mathrm{half},L,n}_{geo,\sigma}$ inspection (cf. Fig. 3) shows that two types of triangles occur: the first type are the triangles $\widetilde{K}$ in $\widetilde{T}\setminus\widetilde{T}_1$ on which one has $\widetilde{r}(\widetilde{x},\widetilde{y})\sim\widetilde{y}$ (uniformly in L, n). The second type are the triangles in $\widetilde{T}_1$. For the first type, we have from (3.22) the regularity assertion (with suitably adjusted C_u, γ, α independent of ε)

$$\forall\widetilde{\mathbf{x}}\in\widetilde{K}\;\forall n\in\mathbb{N}_0:\quad |\nabla^n\widetilde{u}(\widetilde{\mathbf{x}})|\leqslant C_u\gamma^n\max\{n,\varepsilon^{-1}\}^n e^{-\alpha\widetilde{r}(\widetilde{\mathbf{x}})/\varepsilon}.$$

This is the same regularity assumption that underlies the proof of part (ii) of the lemma so that the same arguments can be brought to bear as in the case of part (ii). For the second type of triangles, i.e., $\widetilde{K}\subset\widetilde{T}_1\subset(0,\sigma^L)^2$, the resolution assumption (3.23) implies for the element size $h_{\widetilde{K}}\lesssim\sigma^L\lesssim\varepsilon$. Hence, again Lemma 3.1, (v) is applicable and yields the desired exponential approximation.

Approximation of $\widetilde{u}$ on rectangular elements $\widetilde{K}$: The case of rectangular elements $\widetilde{K}$ with side lengths $h_{\widetilde{K},x}$, $h_{\widetilde{K},y}$ is similar to the case of triangles. We note that the patches $\widetilde{\mathscr{T}}^{\mathsf{BL},L}_{geo,\sigma}$ and $\widetilde{\mathscr{T}}^{\mathsf{M},\mathrm{half},L,n}_{geo,\sigma}$ are such that $h_{\widetilde{K},\widetilde{y}}\leqslant h_{\widetilde{K},\widetilde{x}}\leqslant 1$. The anisotropic scaling from $\widetilde{K}$ to $\widehat{K}$ and the regularity assumption (3.22) show that the pull-back $\widehat{u}$ to $\widehat{K}$ satisfies for all $(m,n)\in\mathbb{N}_0^2$

$$\|\partial_{\widehat{x}}^m\partial_{\widehat{y}}^n\widehat{u}\|_{L^\infty(\widehat{K})}\leqslant Ce^{-\alpha\,\mathrm{dist}(\widetilde{K},\{\widetilde{y}=0\})/\varepsilon}h_{\widetilde{K},\widetilde{x}}^m h_{\widetilde{K},\widetilde{y}}^n\gamma^{n+m}m!\max\{n+1,\varepsilon^{-1}\}^n\,.$$

That is, $\widehat{u}$ satisfies the analytic regularity condition (3.2) with $\varepsilon_y=\varepsilon$, $\varepsilon_x=1$, $h_x=h_{\widetilde{K},\widetilde{x}}$, $h_y=h_{\widetilde{K},\widetilde{y}}$ and $C_u=Ce^{-\alpha\,\mathrm{dist}(\widetilde{K},\{\widetilde{y}=0\})/\varepsilon}$. We observe that the resolution condition (3.3) can be achieved if $\widetilde{K}$ touches the line $\{\widetilde{y}=0\}$ in view of (3.23) provided that $q\geqslant q_0\geqslant 1$ for suitable q_0 (depending on c_1, σ, γ). If $\widetilde{K}$ does not touch the line $\{\widetilde{y}=0\}$, then two cases may occur: If the resolution condition (3.3) is still satisfied then we obtain again exponential convergence. If not, we note that $h_{\widetilde{K},\widetilde{y}}\leqslant h_{\widetilde{K},\widetilde{x}}$ and that we may assume $h_{\widetilde{K},\widetilde{x}}/q\leqslant\delta/2$ by assuming $q\geqslant q_0\geqslant 1$ (note: trivially, $h_{\widetilde{K},\widetilde{x}}\leqslant 1$ so that $q_0\geqslant 2/\delta$ will work). Furthermore, Lemma 2.1, (iii) reveals again that $\mathrm{dist}(\widetilde{K},\{\widetilde{y}=0\})\geqslant c_3h_{\widetilde{K},\widetilde{y}}$; since $h_{\widetilde{K},\widetilde{y}}/(\varepsilon q)\geqslant\delta/2$ we get $\mathrm{dist}(\widetilde{K},\{\widetilde{y}=0\})/\varepsilon\geqslant qc_3\delta/2$. Hence, $\exp(-\alpha\,\mathrm{dist}(\widetilde{K},\{\widetilde{y}=0\})/\varepsilon)\leqslant\exp(-q\alpha c_2\delta/2)$ and we may argue as in the case of triangles that $\widetilde{u}$ is exponentially (in q) small on $\widetilde{K}$. The stability of $\widetilde{\Pi}_q$ given in (3.7) then concludes the argument. □

3.2.3 *hp-FE approximation of corner layer functions.*

LEMMA 3.5 (approximation of corner layer functions) Fix $c_1>0$. Let $\widetilde{\mathscr{T}}\in\{\widetilde{\mathscr{T}}^{\mathsf{M},\mathrm{half},L,n}_{geo,\sigma},\widetilde{\mathscr{T}}^{\mathsf{C},\mathrm{half},n}_{geo,\sigma},\widetilde{\mathscr{T}}^{\mathsf{C},\mathrm{half},\mathrm{flip},n}_{geo,\sigma},\widetilde{\mathscr{T}}^{\mathsf{C},n}_{geo,\sigma},\widetilde{\mathscr{T}}^{\mathsf{T},n}_{geo,\sigma}\}$. Let $\widetilde{\mathscr{T}}'\subset\widetilde{\mathscr{T}}$ and let $\mathscr{O}:=\mathrm{interior}\big(\cup\{\widetilde{\widetilde{K}}\,|\,\widetilde{K}\in\widetilde{\mathscr{T}}'\}\big)$ be the union of the elements of $\widetilde{\mathscr{T}}'$. Let $\widetilde{u}$ be analytic on $\mathscr{O}$ and satisfy for some $\beta\in[0,1)$, $\varepsilon\in(0,1]$, C_u, γ, $\alpha>0$

$$\forall\widetilde{\mathbf{x}}\in\mathscr{O}\quad\forall p\in\mathbb{N}_0:\;\;|\nabla^p\widetilde{u}(\widetilde{\mathbf{x}})|\leqslant C_u\varepsilon^{\beta-1}\gamma^p(\widetilde{r}(\widetilde{\mathbf{x}}))^{1-\beta-p}p!e^{-\alpha\widetilde{r}(\widetilde{\mathbf{x}})/\varepsilon}. \tag{3.32}$$

Assume that $n\in\mathbb{N}$ is such that the scale resolution condition

$$\sigma^n\leqslant c_1\varepsilon. \tag{3.33}$$

is satisfied. Then there are constants C, $b>0$ depending only on γ, α, c_1, σ, and β (in particular, they are independent of ε, q, n, L) such that for all $q\in\mathbb{N}$

$$\|\widetilde{u}-\widetilde{\Pi}_q\widetilde{u}\|_{L^\infty(\mathscr{O})}\leqslant CC_u\left(e^{-bq}+q^4\varepsilon^{\beta-1}\sigma^{n(1-\beta)}\right), \tag{3.34}$$

$$\|\widetilde{u}-\widetilde{\Pi}_q\widetilde{u}\|_{L^2(\mathscr{O})}+\varepsilon\|\nabla(\widetilde{u}-\widetilde{\Pi}_q\widetilde{u})\|_{L^2(\mathscr{O})}\leqslant CC_u\varepsilon\left(e^{-bq}+q^4\varepsilon^{\beta-1}\sigma^{n(1-\beta)}\right). \tag{3.35}$$

In the estimates (3.34), (3.35) the term $q^4\varepsilon^{\beta-1}\sigma^{n(1-\beta)}$ can be dropped if $\mathscr{O}$ does not touch $\mathbf{0}$.

Proof. The approximation of functions of corner layer type $\widetilde{u}$ proceeds structurally along the same lines as in the case of the singularity functions in Lemma 3.3. We distinguish between the elements touching $\mathbf{0}$ and the remaining ones.

$\widetilde{K}$ touches $\mathbf{0}$: Selecting $\widetilde{\beta}\in(\beta,1)$ we obtain by arguing as in (3.14)

$$\|\widetilde{u}-\widetilde{\Pi}_q\widetilde{u}\|_{L^\infty(\widetilde{K})}+\|\nabla(\widetilde{u}-\widetilde{\Pi}_q\widetilde{u})\|_{L^2(\widetilde{K})}\lesssim h_{\widetilde{K}}^{1-\widetilde{\beta}}q^4\|\widetilde{r}^{\widetilde{\beta}}\nabla^2\widetilde{u}\|_{L^2(\widetilde{K})}\lesssim q^4(h_{\widetilde{K}}/\varepsilon)^{1-\beta}. \tag{3.36}$$

Since $h_{\widetilde{K}}\lesssim\sigma^n$ for elements $\widetilde{K}$ touching $\mathbf{0}$, their contributions lead to the term $q^4\varepsilon^{\beta-1}\sigma^{n(1-\beta)}$.

K does not touch $\mathbf{0}$: We distinguish between triangular and rectangular elements.

Step 1: $\widetilde{K}$ is a triangular element: As in the case of the approximation in Lemma 3.3, we get from Lemma 3.1, (v) and scaling that (for suitably adjusted C, α)

$$\|\widetilde{u}-\widetilde{\Pi}_q\widetilde{u}\|_{L^\infty(\widetilde{K})}+\|\nabla(\widetilde{u}-\widetilde{\Pi}_q\widetilde{u})\|_{L^2(\widetilde{K})}\leqslant C(h_{\widetilde{K}}/\varepsilon)^{1-\beta}e^{-bq}e^{-\alpha h_{\widetilde{K}}/\varepsilon}. \tag{3.37}$$

Step 2: $\widetilde{K}$ is a rectangular element: We recall $h_{\widetilde{K},\widetilde{y}}\leqslant h_{\widetilde{K},\widetilde{x}}\leqslant 1$. By Lemma 2.1, (iv) we have $\widetilde{r}(\cdot)\sim h_{\widetilde{K},\widetilde{x}}$ on $\widetilde{K}$. As in the case of Lemma 3.3 we observe for the pull-back to the reference element $\widehat{K}$

$$\forall(m,n)\in\mathbb{N}_0^2\colon\quad \|\partial_{\widehat{x}}^m\partial_{\widehat{y}}^n\widehat{u}\|_{L^\infty(\widehat{K})}\leqslant C(h_{\widetilde{K},\widetilde{x}}/\varepsilon)^{1-\beta}e^{-\alpha h_{\widetilde{K},\widetilde{x}}/\varepsilon}\gamma^{n+m}n!m!h_{\widetilde{K},\widetilde{x}}^{m-(m+n)}h_{\widetilde{K},\widetilde{y}}^n.$$

Using Lemma 3.2, (iv) (with $\varepsilon_x=\varepsilon_y=1$ and $h_y=h_{\widetilde{K},\widetilde{y}}/h_{\widetilde{K},\widetilde{x}}$, $h_x=1$ there), we arrive at

$$\|\widehat{u}-\widehat{\Pi}_q^{\square}\widehat{u}\|_{L^\infty(\widehat{K})}\leqslant C(h_{\widetilde{K}}/\varepsilon)^{1-\beta}e^{-bq}e^{-\alpha h_{\widetilde{K},\widetilde{x}}/\varepsilon}, \tag{3.38}$$

$$\|\partial_{\widehat{x}}(\widehat{u}-\widehat{\Pi}_q^{\square}\widehat{u})\|_{L^\infty(\widehat{K})}\leqslant C(h_{\widetilde{K}}/\varepsilon)^{1-\beta}e^{-bq}e^{-\alpha h_{\widetilde{K},\widetilde{x}}/\varepsilon}, \tag{3.39}$$

$$\|\partial_{\widehat{y}}(\widehat{u}-\widehat{\Pi}_q^{\square}\widehat{u})\|_{L^\infty(\widehat{K})}\leqslant C(h_{\widetilde{K}}/\varepsilon)^{1-\beta}\frac{h_{\widetilde{K},\widetilde{y}}}{h_{\widetilde{K},\widetilde{x}}}e^{-bq}e^{-\alpha h_{\widetilde{K},\widetilde{x}}/\varepsilon}. \tag{3.40}$$

Step 3 (L^∞-bound): Since $\sup_{t>0}t^{1-\beta}e^{-t}<\infty$, the L^∞-estimates follow easily from (3.36), (3.37), (3.38).

Step 4 (energy norm estimate): Proceeding as in Step 3 of the proof of Lemma 3.3 we set $e_{\widetilde{K}}:=\widetilde{u}-\widetilde{\Pi}_q\widetilde{u}$ and get, using $h_{\widetilde{K}}\lesssim\varepsilon$ for the elements abutting on $\mathbf{0}$:

$$\begin{aligned}&\sum_{\widetilde{K}\colon\widetilde{K}\text{ abuts on }\mathbf{0}}\|e_{\widetilde{K}}\|_{L^2(\widetilde{K})}^2+\varepsilon^2\|\nabla e_{\widetilde{K}}\|_{L^2(\widetilde{K})}^2\\ &\overset{(3.36)}{\lesssim} q^8\sum_{\widetilde{K}\colon\widetilde{K}\text{ abuts on }\mathbf{0}}(h_{\widetilde{K}}^2+\varepsilon^2)(h_{\widetilde{K}}/\varepsilon)^{2(1-\beta)}\lesssim q^8\varepsilon^{2\beta}\sigma^{2n(1-\beta)}.\end{aligned}$$

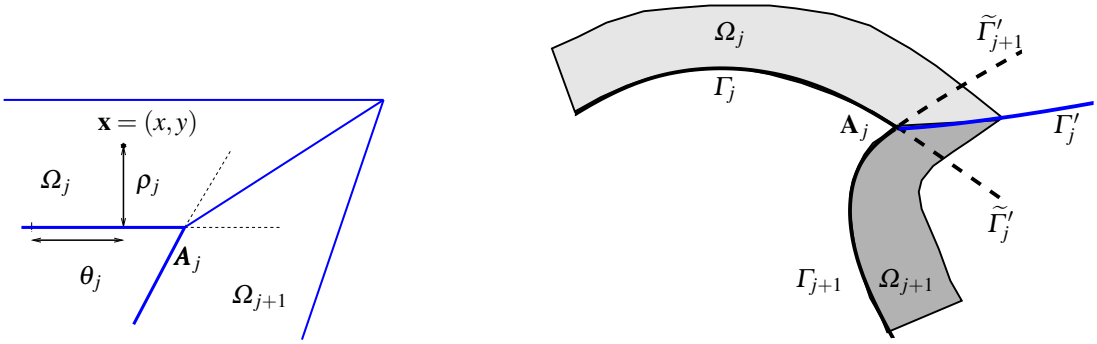

FIG. 6. Left: boundary fitted coordinates $\psi_j : (\rho_j, \theta_j) \mapsto (x, y)$. Right: typical situation at a reentrant corner: boundary fitted coordinates (ρ_j, θ_j) and $(\rho_{j+1}, \theta_{j+1})$ are valid in the regions Ω_j, Ω_{j+1}, respectively. $\widetilde{\Gamma}_j$ and $\widetilde{\Gamma}_{j+1}$ are analytic continuations of Γ_j, Γ_{j+1}. The analytic arc Γ'_j is such that the angles $\angle(\Gamma'_j, \Gamma_j)$ and $\angle(\Gamma_{j+1}, \Gamma'_j)$ are both less than π.

For the remaining elements, we consider the triangular elements and the rectangular ones. In both cases, we employ the simple observation

$$\|e_{\widetilde{K}}\|_{L^2(\widetilde{K})} \lesssim h_{\widetilde{K}} \|e_{\widetilde{K}}\|_{L^\infty(\widetilde{K})} = \varepsilon \frac{h_{\widetilde{K}}}{\varepsilon} \|e_{\widetilde{K}}\|_{L^\infty(\widetilde{K})}. \tag{3.41}$$

The sum over all triangles, collected in $\widetilde{\mathscr{T}}^{\triangle}$, yields by combining (3.37) and (3.41) with Lemma 2.1, (viii)

$$\sum_{\widetilde{K} \in \widetilde{\mathscr{T}}^{\triangle}} \|e_{\widetilde{K}}\|^2_{L^2(\widetilde{K})} + \varepsilon^2 \|e_{\widetilde{K}}\|^2_{H^1(\widetilde{K})} \lesssim \varepsilon^2 e^{-2bq}.$$

Likewise, the sum over all rectangular elements, collected in $\widetilde{\mathscr{T}}^{\square}$, yields by combining Lemma 2.1, (ix) with (3.38), (3.41) for the L^2-part and with (3.39), (3.40) for the H^1-part

$$\sum_{\widetilde{K} \in \widetilde{\mathscr{T}}^{\square}} \|e_{\widetilde{K}}\|^2_{L^2(\widetilde{K})} + \varepsilon^2 \|e_{\widetilde{K}}\|^2_{H^1(\widetilde{K})} \lesssim \varepsilon^2 e^{-2bq}.$$

This concludes the proof. □

4. *hp*-FE approximation of singularly perturbed problems on geometric boundary layer meshes

The principal result of the present paper is a robust, exponential approximation result for solutions of the singular perturbation problem (1.1), (1.2) in curvilinear polygonal domains from spaces based on geometric boundary layer meshes that are able to resolve the length scales present in the problem. The meshes are independent of ε but subject to the (weak) scale resolution condition (4.1).

THEOREM 4.1 Let the Lipschitz domain $\Omega \subset \mathbb{R}^2$ be a curvilinear polygon with J vertices as described in Section 1.2. Let A, c, f satisfy (1.2). Fix $c_1 > 0$. Let $\mathscr{T}^{L,n}_{geo,\sigma}$ be a geometric boundary layer mesh in sense of Definition 2.2.

Then there are constants $C, b > 0$, $\beta \in [0, 1)$ depending solely on the data A, c, f, Ω, on the parameter c_1, on the (fixed) macro-triangulation $\mathscr{T}^{\mathscr{M}}$, and on $\sigma \in (0, 1)$ such that the following holds: If $\varepsilon \in (0, 1]$

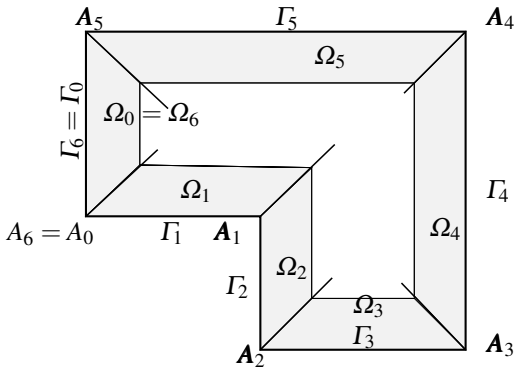

FIG. 7. The subdomains Ω_j on which the boundary layer expansion $u_\varepsilon^{\mathsf{BL}}$ is defined in terms of boundary fitted coordinates (ρ_j, θ_j).

and L satisfy the scale resolution condition

$$\frac{\sigma^L}{\varepsilon} \leqslant c_1, \tag{4.1}$$

then for every q, $n \in \mathbb{N}$ the solution $u_\varepsilon \in H_0^1(\Omega)$ of (1.1) can be approximated from $S_0^q(\Omega, \mathscr{T}_{geo,\sigma}^{L,n})$ such that

$$\inf_{v \in S_0^q(\Omega, \mathscr{T}_{geo,\sigma}^{L,n})} \|u_\varepsilon - v\|_{\varepsilon,\Omega} \leqslant C q^9 \left[\varepsilon^\beta \sigma^{(1-\beta)n} + e^{-bq} \right], \tag{4.2}$$

$$N := \dim S_0^q(\Omega, \mathscr{T}_{geo,\sigma}^{L,n}) \leqslant C\big(L^2 q^2 \operatorname{card} \mathscr{T}^{\mathscr{M}} + nq^2 J\big). \tag{4.3}$$

Proof. Before proving the result, let us comment on the scale resolution (4.1) and its relation to previous scale resolution conditions (3.9), (3.33), and (3.23). Condition (4.1) ensures that L layers of anisotropic refinement towards the boundary are performed, which is the condition (3.23) needed to resolve functions of boundary layer type. Since $n \geqslant L$ (by Def. 2.2), condition (4.1) also enforces the condition (3.33), which provides the approximation of corner layer functions. Finally, the situation (3.9) is of a different nature as in that case, the polynomial degree is so large that already very coarse meshes can resolve the boundary layers.

We employ the analytic, parametric regularity theory for the solution u_ε presented in (Melenk, 2002, Thms. 2.3.1, 2.3.4). The infimum in (4.2) is estimated with the aid of the interpolation operator Π_q that is defined elementwise by

$$(\Pi_q u)|_K \circ F_K := \begin{cases} \widehat{\Pi}_q^{\triangle}(u \circ F_K) & \text{if } K \text{ is a triangle} \\ \widehat{\Pi}_q^{\square}(u \circ F_K) & \text{if } K \text{ is a rectangle.} \end{cases}$$

Here, the operator $\widehat{\Pi}_q^{\triangle}$ is defined in Lemma 3.1 and the operator $\widehat{\Pi}_q^{\square}$ in Lemma 3.2. Since $\widehat{\Pi}_q^{\triangle}$ and $\widehat{\Pi}_q^{\square}$ reduce to the Gauss-Lobatto interpolation operator on the edges of the reference element, the operator Π_q indeed maps into $S_0^q(\Omega, \mathscr{T}_{geo,\sigma}^{L,n})$. We recall that the element maps F_K have the form

$$F_K = F_{K^{\mathscr{M}}} \circ A_K,$$

where $A_K : \widehat{K} \to \widetilde{K} := A_K(\widehat{K}) = F_{K^{\mathscr{M}}}^{-1}(K) \subset \widetilde{S}$ is an affine bijection. Indeed, for triangular elements it is clear that A_K is affine and for rectangular elements, this follows from the special form of the reference patches (cf. also Lemma 2.1, (i)).

The notation $\widehat{u}$ denotes the pull-back of u to the reference element, i.e., $\widehat{u} := u|_K \circ F_K$ whereas $\widetilde{u} := (u \circ F_{K^{\mathscr{M}}})|_{\widetilde{K}} = \widehat{u} \circ A_K^{-1}$ is the corresponding function on $\widetilde{K}$. We recall the notation $\widetilde{\Pi}_q$ from (3.6) and note that on a macro-element $K^{\mathscr{M}}$ we have

$$(\Pi_q u) \circ F_{K^{\mathscr{M}}} = \widetilde{\Pi}_q \widetilde{u}.$$

For $k \in \mathbb{N}_0$ we have for all elements $K \subset K^{\mathscr{M}}$ with $\widetilde{K} = F_{K^{\mathscr{M}}}^{-1}(K)$

$$\forall v \in H^k(K): \quad \|v \circ F_{K^{\mathscr{M}}}\|_{H^k(\widetilde{K})} \sim \|v\|_{H^k(K)}, \tag{4.4a}$$

$$\forall v \in W^{k,\infty}(K): \quad \|v \circ F_{K^{\mathscr{M}}}\|_{W^{k,\infty}(\widetilde{K})} \sim \|v\|_{W^{k,\infty}(K)}, \tag{4.4b}$$

where in both cases the constants implied in $\sim$ depend solely on k and the macro-element $K^{\mathscr{M}}$. The equivalences (4.4) show that the approximation error $v - \Pi_q v$ on K is equivalent to the corresponding error $\widetilde{v} - \widetilde{\Pi}_q \widetilde{v}$ on $\widetilde{K}$.

The approximation theory distinguishes between the "asymptotic case" $q\varepsilon \geqslant \kappa$ of large polynomial degree q and the "preasymptotic case" $q\varepsilon \leqslant \kappa$, where the parameter $\kappa > 0$ (depending only on A, c, f, Ω, the macro-triangulation, and σ) is of size $O(1)$ and will be determined in the course of the analysis of the "asymptotic case" in Step I.

Step I: Asymptotic case $q\varepsilon \geqslant \kappa$. We consider mesh patches $K^{\mathscr{M}}$ that abut on a vertex $\boldsymbol{A}_j$ and those with a positive distance from the vertices separately in Steps I.1 and I.2.

Step I.1: $K^{\mathscr{M}}$ abuts on a vertex $\boldsymbol{A}_j$: The regularity of (Melenk, 2002, Thm. 2.3.1) asserts the existence of C, $\gamma > 0$, $\beta_j \in [0,1)$ such that with $r_j(\cdot) := \operatorname{dist}(\cdot, \boldsymbol{A}_j)$, there holds for every $p \in \mathbb{N}_0$ and for every $0 < \varepsilon \leqslant 1$

$$|\nabla^p (u_\varepsilon(\cdot) - u_\varepsilon(\boldsymbol{A}_j))| \leqslant C\gamma^p \varepsilon^{-1} \min\{1, r_j(\cdot)/\varepsilon\}^{1-\beta_j} (r_j(\cdot))^{-p} \max\{p+1, r_j(\cdot)/\varepsilon\}^{p+1}. \tag{4.5}$$

Recall from (3.5) that $\widetilde{r}(\cdot) = \operatorname{dist}(\cdot, \mathbf{0})$. Set $\widetilde{u}_\varepsilon := u_\varepsilon \circ F_{K^{\mathscr{M}}}$. Note $F_{K^{\mathscr{M}}}(\mathbf{0}) = \boldsymbol{A}_j$ and $\widetilde{r}(\widetilde{\mathbf{x}}) \sim r_j(F_{K^{\mathscr{M}}}(\widetilde{\mathbf{x}}))$. The analyticity of $F_{K^{\mathscr{M}}}$ and Lemma A.2 imply, for suitably modified constants C, γ independent of $\varepsilon \in (0,1]$, for every $p \in \mathbb{N}_0$ holds on $\widetilde{K}$

$$|\nabla^p (\widetilde{u}_\varepsilon(\cdot) - \widetilde{u}(\mathbf{0}))| \leqslant C\gamma^p \varepsilon^{-1} \min\{1, \widetilde{r}/\varepsilon\}^{1-\beta_j} (\widetilde{r}(\cdot))^{-p} \max\{p+1, \widetilde{r}(\cdot)/\varepsilon\}^{p+1}. \tag{4.6}$$

Lemma 3.3 then yields

$$\|\widetilde{u}_\varepsilon - \widetilde{\Pi}_q \widetilde{u}_\varepsilon\|_{L^\infty(K^{\mathscr{M}})} + \|\nabla(\widetilde{u}_\varepsilon - \widetilde{\Pi}_q \widetilde{u}_\varepsilon)\|_{L^\infty(K^{\mathscr{M}})} \leqslant Cq^9 \left(\sigma^{(1-\beta_j)n} + e^{-bq}\right)$$

provided that κ is chosen sufficiently large (depending on γ).

Step I.2: $K^{\mathscr{M}}$ does not abut on a vertex $\boldsymbol{A}_j$: (Melenk, 2002, Thm. 2.3.1) asserts

$$\forall \mathbf{x} \in K^{\mathscr{M}} \quad \forall p \in \mathbb{N}_0: \quad |\nabla^p u(\mathbf{x})| \leqslant C\gamma^p \max\{p+1, \varepsilon^{-1}\}^{p+2} \tag{4.7}$$

for constants C, $\gamma > 0$ independent of $\varepsilon \in (0,1]$. Since $K^{\mathscr{M}}$ is a trivial patch, it consists of a single (curvilinear) quadrilateral. The analyticity of $F_{K^{\mathscr{M}}} = F_K$ and Lemma A.2 imply, for suitably modified C, γ independent of $\varepsilon \in (0,1]$, that

$$\forall \widehat{\mathbf{x}} \in \widehat{S} \quad \forall p \in \mathbb{N}_0: \quad |\nabla^p \widehat{u}(\widehat{\mathbf{x}})| \leqslant C\gamma^p \max\{p+1, \varepsilon^{-1}\}^{p+2}. \tag{4.8}$$

Lemma 3.2 then implies that there are C, $b > 0$ such that for sufficiently large, fixed κ and for every $\varepsilon \in (0,1]$ and every $q \in \mathbb{N}$ holds

$$\|\widehat{u} - \widehat{\Pi}_q \widehat{u}\|_{L^\infty(K^{\mathscr{M}})} + \|\nabla(\widehat{u} - \widehat{\Pi}_q \widehat{u})\|_{L^\infty(\widehat{S})} \leqslant Ce^{-bq} .$$

Step I.3: Combining the approximation results of Steps I.1, I.2 for the finitely many patches leads to the desired estimate (4.2).

Step II: Preasymptotic case $q\varepsilon \leqslant \kappa$. The parameter κ has been fixed in Step I through the appeal to Lemmas 3.3 and 3.2. In the regime $q\varepsilon \leqslant \kappa$, we employ the regularity theory of (Melenk, 2002, Thm. 2.3.4), which furnishes the decomposition $u_\varepsilon = w_\varepsilon + \chi^{\mathsf{BL}} u_\varepsilon^{\mathsf{BL}} + \chi^{\mathsf{CL}} u_\varepsilon^{\mathsf{CL}} + r_\varepsilon$ into a smooth part w_ε, a boundary layer part $u_\varepsilon^{\mathsf{BL}}$, a corner layer part $u_\varepsilon^{\mathsf{CL}}$, and a small remainder r_ε; the functions χ^{BL}, χ^{CL} are suitable localizations near the boundary and the vertices of Ω. We approximate each of these four contributions in turn.

Step II.1: Approximation of w_ε. By (Melenk, 2002, Thm. 2.3.4) the smooth part w_ε is analytic on $\overline{\Omega}$ with constants independent of ε. Therefore, one can show $\|w_\varepsilon - \Pi_q w_\varepsilon\|_{W^{1,\infty}(\Omega)} \leqslant Ce^{-bq}$ using similar techniques as in the asymptotic case above (essentially, setting $\varepsilon = 1$ there and ignoring the special treatment of the elements abutting on the vertices of Ω).

Step II.2: Approximation of $\chi^{\mathsf{BL}} u_\varepsilon^{\mathsf{BL}}$.

Step II.2.a: Regularity of $u_\varepsilon^{\mathsf{BL}}$: The regularity of $u_\varepsilon^{\mathsf{BL}}$ in (Melenk, 2002, Thm. 2.3.4) is described in terms of boundary fitted coordinates (cf. Fig. 6). Associated with each edge Γ_j are fitted coordinates (ρ_j, θ_j), where ρ_j is the distance from the analytic continuation $\widetilde{\Gamma}_j$ of the boundary arc Γ_j, and θ_j is a parametrization of Γ_j. The map $\psi_j : (\rho_j, \theta_j) \mapsto (x,y) \in \Omega$ is analytic with an analytic inverse. An analytic arc Γ_j' emanates from each vertex $\boldsymbol{A}_j$, which can be chosen arbitrarily but is assumed to be such that the angles between Γ_j and Γ_j' and between Γ_{j+1} and Γ_j' are both less than π. Condition 8 of Definition 2.2 ensures that Γ_j' can be chosen to be a meshline of a boundary layer mesh since it can be chosen as the image of an edge of $\widetilde{S}$ or a diagonal of $\widetilde{S}$ under a patch map.

The regions $\Omega_j \subset \{\mathbf{x} \in \Omega \mid \operatorname{dist}(\mathbf{x}, \Gamma_j) < \delta\}$ for a sufficiently small δ are confined by the lines Γ_j, Γ_j', and Γ_{j-1}' as shown in Fig. 7. By (Melenk, 2002, Thm. 2.3.4), the function $u_\varepsilon^{\mathsf{BL}}$ is analytic on each Ω_j and satisfies there, for constants C, γ, $\alpha > 0$ independent of $\varepsilon \in (0,1]$ and all $(m,n) \in \mathbb{N}_0$,

$$\begin{aligned} |\partial_{\rho_j}^n \partial_{\theta_j}^m u_\varepsilon^{\mathsf{BL}} \circ \psi_j(\rho_j, \theta_j)| &\overset{\text{(Melenk, 2002, Thm. 2.3.4)}}{\leqslant} C\varepsilon^{-n} \gamma^{n+m} m! e^{-\alpha\rho_j/\varepsilon} \\ &\leqslant C\gamma^{n+m} \max\{n+m, \varepsilon^{-1}\}^{n+m} e^{-\alpha\rho_j/\varepsilon} . \end{aligned} \tag{4.9}$$

Finally, the cut-off function χ^{BL} is supported by $\cup_j \overline{\Omega_j}$ and is identically 1 near $\partial\Omega$.

Step II.2.b: Approximation of $\chi^{\mathsf{BL}} u_\varepsilon^{\mathsf{BL}}$ far from $\partial\Omega$: In the interest of simplicity of notation, we make the assumption that patches $K^{\mathscr{M}}$ touching $\partial\Omega$ are fully contained in the tubular neighborhood $\cup_j \overline{\Omega_j}$ of $\partial\Omega$. Since patches $K^{\mathscr{M}}$ not touching $\partial\Omega$ have a positive distance from $\partial\Omega$, the function $\chi^{\mathsf{BL}} u_\varepsilon^{\mathsf{BL}}$ is exponentially small (in $1/\varepsilon$) there; in view of the stability (3.7) (and thus the stability of Π_q) $\|\chi^{\mathsf{BL}} u_\varepsilon^{\mathsf{BL}} - \Pi_p(\chi^{\mathsf{BL}} u_\varepsilon^{\mathsf{BL}})\|_{W^{1,\infty}(K)} \leqslant Ce^{-b/\varepsilon}$ for $K \in K^{\mathscr{M}}$. Since $q/\kappa \leqslant 1/\varepsilon$ the error contribution of these patches is controlled in the desired fashion.

Step II.2.c: Approximation of $\chi^{\mathsf{BL}} u_\varepsilon^{\mathsf{BL}}$ near $\partial\Omega$: Let $K^{\mathscr{M}}$ be a patch touching $\partial\Omega$. Consider, for a fixed j the pull-back $F_{K^{\mathscr{M}}}^{-1}(K^{\mathscr{M}} \cap \Omega_j)$. By the assumptions of the boundary layer mesh (Def. 2.2) this pull back is either empty, the full square $\widetilde{S}$, half the square $\widetilde{T} = \{\widetilde{\mathbf{x}} = (\widetilde{x}, \widetilde{y}) \,|\, 0 < \widetilde{x} < 1, 0 < \widetilde{y} < \widetilde{x}\}$, or the other half $T^{\text{flip}} = \{\widetilde{\mathbf{x}} = (\widetilde{x}, \widetilde{y}) \,|\, 0 < \widetilde{x} < 1, \widetilde{x} < \widetilde{y} < 1\}$.

To fix ideas, let us assume that $K^{\mathscr{M}}$ is a mixed patch. The reference mixed patch restricted to $\widetilde{T}$ is the half-patch $\widetilde{\mathscr{T}}^{\mathsf{M},\mathrm{half},L,n}$ and its restriction to T^{flip} is $\widetilde{\mathscr{T}}^{\mathsf{C},\mathrm{half},\mathrm{flip},n}$. We approximate $(\chi^{\mathsf{BL}}u_\varepsilon^{\mathsf{BL}})\circ F_{K^{\mathscr{M}}}$ on these two parts separately, starting with the approximation on $\widetilde{T}$. The assumptions on boundary layer meshes (Def. 2.2) allow us to assume that $F_{K^{\mathscr{M}}}(\widetilde{T})\subset\Omega_j$ for some j. We recall that $F_{K^{\mathscr{M}}}$ maps the edge $\{\widetilde{y}=0\}$ of $\widetilde{T}$ to (a subset of) $\partial\Omega$, which corresponds to $\rho_j=0$ in the boundary fitted coordinates. The shape-regularity of $F_{K^{\mathscr{M}}}$ implies that $\psi_j^{-1}\circ F_{K^{\mathscr{M}}}$ has the form

$$\widetilde{T}\ni(\widetilde{x},\widetilde{y})\mapsto(\rho_j,\theta_j)=(\widetilde{y}\rho(\widetilde{x},\widetilde{y}),\theta(\widetilde{x},\widetilde{y})) \tag{4.10}$$

for a pair of functions ρ, θ with $\rho\geqslant\rho_0>0$. The analyticity of ψ_j^{-1} and $F_{K^{\mathscr{M}}}$ implies that ρ and θ are in fact analytic on $\overline{\overline{\widetilde{T}}}$. Hence, the transformed function

$$\widetilde{u}_\varepsilon^{\mathsf{BL}}:=u_\varepsilon^{\mathsf{BL}}\circ F_{K^{\mathscr{M}}}=u_\varepsilon^{\mathsf{BL}}\circ\psi_j\circ(\psi_j^{-1}\circ F_{K^{\mathscr{M}}}) \tag{4.11}$$

admits by Lemma A.1 and (4.9) the analytic regularity

$$\forall(m,n)\in\mathbb{N}_0^2\quad\forall(\widetilde{x},\widetilde{y})\in\widetilde{T}\colon\ \ |\partial_{\widetilde{x}}^m\partial_{\widetilde{y}}^n\widetilde{u}_\varepsilon^{\mathsf{BL}}(\widetilde{x},\widetilde{y})|\leqslant C\gamma^{m+n}m!\max\{n+1,\varepsilon^{-1}\}^n e^{-b\widetilde{y}/\varepsilon}, \tag{4.12}$$

where the constants C, γ, $b>0$ are independent of $\varepsilon\in(0,1]$. We decompose the set of elements $\widetilde{\mathscr{T}}^{\mathsf{M},\mathrm{half},L,n}$ into two sets $\widetilde{\mathscr{T}_1}:=\{\widetilde{K}\in\widetilde{\mathscr{T}}_{geo,\sigma}^{\mathsf{M},\mathrm{half},L,n}\,|\,\widetilde{\chi}^{\mathsf{BL}}|_{\widetilde{K}}\equiv 1\}$ and $\widetilde{\mathscr{T}_2}:=\widetilde{\mathscr{T}}_{geo,\sigma}^{\mathsf{M},\mathrm{half},L,n}\setminus\widetilde{\mathscr{T}_1}$. For the elements of $\widetilde{\mathscr{T}_1}$, Lemma 3.4, (i) and (4.12) give that there are C, $b>0$ such that for every $q\in\mathbb{N}$ and every $\widetilde{K}\in\widetilde{\mathscr{T}_1}$

$$\|\widetilde{\chi}^{\mathsf{BL}}\widetilde{u}_\varepsilon^{\mathsf{BL}}-\widetilde{\Pi}_q(\widetilde{\chi}^{\mathsf{BL}}\widetilde{u}_\varepsilon^{\mathsf{BL}})\|_{L^\infty(\widetilde{K})}+\varepsilon\|\nabla(\widetilde{\chi}^{\mathsf{BL}}\widetilde{u}_\varepsilon^{\mathsf{BL}}-\widetilde{\Pi}_q(\widetilde{\chi}^{\mathsf{BL}}\widetilde{u}_\varepsilon^{\mathsf{BL}}))\|_{L^\infty(\widetilde{K})}\leqslant Ce^{-bq}. \tag{4.13}$$

For the elements of the set $\widetilde{\mathscr{T}_2}$, we use (4.10) to see that $\widetilde{K}\in\widetilde{\mathscr{T}_2}$ implies $\mathrm{dist}(\widetilde{K},\{\widetilde{y}=0\})>c$ for some $c>0$ that depends solely on $F_{K^{\mathscr{M}}}$ and ψ_j. Hence, the smoothness of $\widetilde{\chi}^{\mathsf{BL}}$ and (4.12) provide $\|\widetilde{\chi}^{\mathsf{BL}}\widetilde{u}_\varepsilon^{\mathsf{BL}}\|_{W^{1,\infty}(\widetilde{K})}\leqslant Ce^{-b/\varepsilon}$ for suitable C, $b>0$ and every $\widetilde{K}\in\widetilde{\mathscr{T}_2}$. Hence, the stability properties of $\widetilde{\Pi}_q$ provided in (3.7) and $q/\kappa\leqslant 1/\varepsilon$ imply for all $\widetilde{K}\in\widetilde{\mathscr{T}_2}$

$$\|\widetilde{\chi}^{\mathsf{BL}}\widetilde{u}_\varepsilon^{\mathsf{BL}}-\widetilde{\Pi}_q(\widetilde{\chi}^{\mathsf{BL}}\widetilde{u}_\varepsilon^{\mathsf{BL}})\|_{L^\infty(\widetilde{K})}+\varepsilon\|\nabla(\widetilde{\chi}^{\mathsf{BL}}\widetilde{u}_\varepsilon^{\mathsf{BL}}-\widetilde{\Pi}_q(\widetilde{\chi}^{\mathsf{BL}}\widetilde{u}_\varepsilon^{\mathsf{BL}}))\|_{L^\infty(\widetilde{K})}\leqslant Ce^{-bq}. \tag{4.14}$$

Let us now sketch the arguments for the approximation of $\widetilde{\chi}^{\mathsf{BL}}\widetilde{u}_\varepsilon^{\mathsf{BL}}$ on T^{flip}. For notational simplicity, assume that $F_{K^{\mathscr{M}}}(T^{\mathrm{flip}})\subset\Omega_j$. (If $F_{K^{\mathscr{M}}}(T^{\mathrm{flip}})\subset\Omega_{j'}$ for some different j', then replace j with j' in what follows.) The regularity assertion (4.12) is still valid. Next, one observes that on T^{flip}, one has $\widetilde{y}\sim\widetilde{r}(\widetilde{x},\widetilde{y})=\mathrm{dist}((\widetilde{x},\widetilde{y}),\mathbf{0})$. Hence, recalling (4.12), $\widetilde{u}_\varepsilon^{\mathsf{BL}}$ satisfies, for suitable C, $b>0$ and for all $p\in\mathbb{N}_0$,

$$|\nabla^p\widetilde{u}_\varepsilon^{\mathsf{BL}}(\cdot)|\leqslant C\max\{p+1,\varepsilon^{-1}\}^p e^{-b\widetilde{r}(\cdot)/\varepsilon}\quad\text{ on }T^{\mathrm{flip}}. \tag{4.15}$$

Replacing the appeal to Lemma 3.4, (i) with a reference to Lemma 3.4, (ii), we may argue as above to obtain

$$\|\widetilde{\chi}^{\mathsf{BL}}\widetilde{u}_\varepsilon^{\mathsf{BL}}-\widetilde{\Pi}_q\widetilde{\chi}^{\mathsf{BL}}\widetilde{u}_\varepsilon^{\mathsf{BL}}\|_{L^\infty(T^{\mathrm{flip}})}+\varepsilon\|\nabla(\widetilde{\chi}^{\mathsf{BL}}\widetilde{u}_\varepsilon^{\mathsf{BL}}-\widetilde{\Pi}_q\widetilde{\chi}^{\mathsf{BL}}\widetilde{u}_\varepsilon^{\mathsf{BL}})\|_{L^\infty(T^{\mathrm{flip}})}\leqslant Ce^{-bq}.$$

This concludes the arguments for the approximation of $\widetilde{u}_\varepsilon^{\mathsf{BL}}$ on a mixed patch $\widetilde{\mathscr{T}}_{geo,\sigma}^{\mathsf{M},L,n}$. The approximation on corner patches $\widetilde{\mathscr{T}}_{geo,\sigma}^{\mathsf{C},n}$, tensor patches $\widetilde{\mathscr{T}}_{geo,\sigma}^{\mathsf{T},n}$, or boundary layer patches $\widetilde{\mathscr{T}}_{geo,\sigma}^{\mathsf{BL},L}$ is similar.

Step II.3: Approximation of $\chi^{\mathsf{CL}} u_\varepsilon^{\mathsf{CL}}$: Structurally, the proof is similar to the procedure in Step II.2. From (Melenk, 2002, Thm. 2.3.4) we have in a neighborhood B_j of vertex $\boldsymbol{A}_j$ that $u_\varepsilon^{\mathsf{CL}}$ satisfies on $(B_j \cap \Omega_j) \cup (B_j \cap \Omega_{j+1})$ with $r_j(\cdot) = \operatorname{dist}(\cdot, A_j)$

$$\forall p \in \mathbb{N}_0 : \quad |\nabla^p u_\varepsilon^{\mathsf{CL}}(\cdot)| \leqslant C\gamma^p p! \varepsilon^{\beta_j - 1} (r_j(\cdot))^{1-p-\beta_j} e^{-\alpha r_j(\cdot)/\varepsilon}, \tag{4.16}$$

where C, $\alpha > 0$ and $\beta_j \in [0,1)$ are independent of $\varepsilon \in (0,1]$. Let $K^{\mathscr{M}}$ be a patch abutting on $\boldsymbol{A}_j$. Such a patch has to be either a corner patch or a mixed patch. Then $K^{\mathscr{M}} \cap \Omega_j$ (and similarly $K^{\mathscr{M}} \cap \Omega_{j+1}$) consists of one or two half-patches that are push-forwards of $\widetilde{\mathscr{T}}' \in \{\widetilde{\mathscr{T}}^{\mathsf{M,half},L,n}_{geo,\sigma}, \widetilde{\mathscr{T}}^{\mathsf{C,half},n}_{geo,\sigma}, \widetilde{\mathscr{T}}^{\mathsf{C,half,flip},n}_{geo,\sigma}\}$. For simplicity of exposition, assume that $K^{\mathscr{M}} \subset B_j$. By the analyticity of the patch-map $F_{K^{\mathscr{M}}}$, the shape regularity of $F_{K^{\mathscr{M}}}$ together with $F_{K^{\mathscr{M}}}(\mathbf{0}) = \boldsymbol{A}_j$, and by Lemma A.2, we get that $\widetilde{u}_\varepsilon^{\mathsf{CL}} := u_\varepsilon^{\mathsf{CL}} \circ F_{K^{\mathscr{M}}}$ satisfies on $\mathscr{O} := F_{K^{\mathscr{M}}}^{-1}(K^{\mathscr{M}} \cap \Omega_j)$

$$\forall p \in \mathbb{N}_0 : \quad |\nabla^p \widetilde{u}_\varepsilon^{\mathsf{CL}}(\cdot)| \leqslant C\gamma^p p! \varepsilon^{\beta_j - 1} (\widetilde{r}(\cdot))^{1-p-\beta_j} e^{-\alpha \widetilde{r}(\cdot)/\varepsilon}, \tag{4.17}$$

with possibly adjusted values for C, γ, $\alpha > 0$. We also note that the pull-back $\widetilde{\chi}^{\mathsf{CL}}$ is smooth and identically 1 near $\mathbf{0}$. Hence, using Lemma 3.5 we obtain

$$\begin{aligned} &\|\widetilde{\chi}^{\mathsf{CL}} \widetilde{u}_\varepsilon^{\mathsf{CL}} - \widetilde{\Pi}_q(\widetilde{\chi}^{\mathsf{CL}} \widetilde{u}_\varepsilon^{\mathsf{CL}})\|_{L^2(\mathscr{O})} + \varepsilon \|\nabla\big(\widetilde{\chi}^{\mathsf{CL}} \widetilde{u}_\varepsilon^{\mathsf{CL}} - \widetilde{\Pi}_q(\widetilde{\chi}^{\mathsf{CL}} \widetilde{u}_\varepsilon^{\mathsf{CL}})\big)\|_{L^2(\mathscr{O})} \\ &\quad \leqslant C\left(\varepsilon e^{-bq} + \varepsilon^{\beta_j} q^4 \sigma^{n(1-\beta_j)}\right). \end{aligned}$$

Step II.4: Approximation of r_ε: We approximate r_ε by zero. We note that (Melenk, 2002, Thm. 2.3.4) asserts that $r_\varepsilon|_{\partial\Omega} = 0$ and that $\|r_\varepsilon\|_{H^1(\Omega)} \leqslant Ce^{-b/\varepsilon}$ for suitable C, $b > 0$ independent of $\varepsilon \in (0,1]$. □

COROLLARY 4.1 Assume the hypotheses on Ω and the data A, c, f as in Theorem 4.1. Let $\mathscr{T}^{L,n}_{geo,\sigma}$ be a geometric boundary layer mesh as in Definition 2.2.

Then, for every fixed $0 < \sigma < 1$ and $c_1 > 0$ there exist constants C, $b > 0$ such that, for every $0 < \varepsilon \leqslant 1$, with the choices $q \simeq n \geqslant L \geqslant c_1 |\log \varepsilon|$, the solution $u_\varepsilon \in H^1_0(\Omega)$ of (1.1) can be approximated from $S^q_0(\Omega, \mathscr{T}^{L,n}_{geo,\sigma})$ at an exponential rate:

$$\inf_{v \in S^q_0(\Omega, \mathscr{T}^{L,n}_{geo,\sigma})} \|u_\varepsilon - v\|_{\varepsilon,\Omega} \leqslant C \exp(-b\sqrt[4]{N}), \quad N = \dim(S^q_0(\Omega, \mathscr{T}^{L,n}_{geo,\sigma})).$$

REMARK 4.1 In addition to the approximation in the energy norm in Cor. 4.1, exponential approximation results in the so-called "balanced norm" $\|v\|^2_{\sqrt{\varepsilon}} := \varepsilon \|\nabla v\|^2_{L^2(\Omega)} + \|v\|^2_{L^2(\Omega)}$ (or even in $H^1(\Omega)$) are possible under slightly stronger conditions: for sufficiently large C_1, the constraint $q \simeq n \geqslant L \geqslant C_1 |\log \varepsilon|$ yields

$$\inf_{v \in S^q_0(\Omega, \mathscr{T}^{L,n}_{geo,\sigma})} \|u_\varepsilon - v\|_{\sqrt{\varepsilon},\Omega} \leqslant C \exp(-b'\sqrt[4]{N})$$

for suitable $b' > 0$ since a factor $\varepsilon^{-1/2}$ can be compensated by the exponentially decaying terms $e^{-b\sqrt[4]{N}}$ in Cor. 4.1. ∎

Theorem 4.1 is restricted to $\varepsilon \in (0,1]$. For $\varepsilon \geqslant 1$, (1.1) is a regularly perturbed elliptic boundary value problem and exponential convergence of hp-FEM with mere geometric corner refinement follows by standard results Schwab (1998); Melenk (2002).

PROPOSITION 4.2 Assume the hypotheses on Ω and the data A, c, f as in Theorem 4.1. Let $\mathscr{T}^{L,n}_{geo,\sigma}$ be a geometric boundary layer mesh. Then, there are constants $C, b > 0$, $\beta \in [0,1)$ depending solely on A, c, f, the analyticity properties of the patch maps for the macro-triangulation, and σ such that for any $\varepsilon \geqslant 1$, the solution u_ε of (1.1) satisfies for every $n, L, q \in \mathbb{N}$

$$\inf_{v \in S^q_0(\Omega, \mathscr{T}^{L,n}_{geo,\sigma})} \|u_\varepsilon - v\|_{H^1(\Omega)} \leqslant C\varepsilon^{-2} \left(q^9 \sigma^{(1-\beta)n} + e^{-bq} \right). \tag{4.18}$$

Proof. The solution $u_\varepsilon \in H^1_0(\Omega)$ satisfies

$$-\nabla \cdot (A \nabla u_\varepsilon) + \varepsilon^{-2} c u_\varepsilon = \varepsilon^{-2} f \quad \text{in } H^{-1}(\Omega). \tag{4.19}$$

For $\varepsilon \geqslant 1$, the term $\varepsilon^{-2}c$ represents a regular perturbation and the analytic regularity theory for linear, second order elliptic boundary value problems (e.g. Babuška & Guo (1988) and the references there) is applicable. The resulting regularity assertions are then those employed in the "asymptotic case" in the proof of Theorem 4.1 with $\varepsilon = 1$ there. The factor ε^{-2} in (4.18) is a reflection of the fact that the right-hand side of (4.19) include the factor ε^{-2}. □

5. Numerical experiments

5.1 *ε-independent discretizations for single scale examples*

For $0 < \varepsilon \leqslant 1$ and $f \equiv 1$ we consider the Dirichlet problem: find $u_\varepsilon \in H^1_0(\Omega)$ such that

$$-\varepsilon^2 \Delta u_\varepsilon + u_\varepsilon = f \ \text{ in } \ H^{-1}(\Omega).$$

Here, the domain Ω is either the unit square $\Omega_1 = (0,1)^2$, the so-called "L-shaped domain" $\Omega_2 \subset \mathbb{R}^2$ determined by the vertices $\{(0,0),(1,0),(1,1),(-1,1),(-1,-1),(0,-1)\}$, the square domain with a slit $\Omega_3 = (-1,1)^2 \setminus (-1,0] \times \{0\}$, or the quadrilateral Ω_4 with corners the same as Ω_1 but with curved sides depicted in Figure 11. The curved sides are cubic splines, e.g., one of the sides is the cubic spline going through the points $(0,0)$, $(0.5,0.25)$, and $(1.0,0.0)$. The other three sides are determined by the corners and the additional points $(0.75,0.5)$, $(0.5,0.75)$ and $(0.25,0.5)$.

In Figures 8–11 we show examples of the meshes used in our computations on the four domains. These are constructed using the NGSolve/Netgen package Schöberl (1997). For the square domain $\Omega = \Omega_1$ the resulting mesh is the geometric boundary layer mesh $\mathscr{T}^{L,L}_{geo,\sigma}$ with $L = 4$ and $\sigma = 0.25$. The same parameters are used in NGSolve/Netgen to construct the meshes for the other three domains, with the resulting meshes differing slightly from the strict definition of $\mathscr{T}^{L,L}_{geo,\sigma}$ near the re-entrant corners. Nevertheless, we denote these meshes also by $\mathscr{T}^{L,L}_{geo,\sigma}$ and make use of the finite element spaces $S^q_0(\Omega, \mathscr{T}^{L,L}_{geo,\sigma})$. We also mention that in accordance with Remark 2.2, the meshes shown in Figs. 8–11 do not satisfy requirement 8 of Definition 2.2.

For each $p = 1,2,3,\ldots$, we use the finite element space $S^q_0(\Omega, \mathscr{T}^{L,L}_{geo,\sigma})$ with uniform polynomial order $q = p$ and with $L = p$ refinement levels towards boundaries and corners with refinement factor $\sigma = 0.25$. We denote by $u^h_\varepsilon \in S^p_0(\Omega, \mathscr{T}^{p,p}_{geo,\sigma})$ the corresponding finite element solution. We measure the error in energy norm

$$\text{error} = \left(\varepsilon^2 \|\nabla(u_\varepsilon - u^h_\varepsilon)\|^2_{L^2(\Omega)} + \|u_\varepsilon - u^h_\varepsilon\|^2_{L^2(\Omega)} \right)^{1/2}, \tag{5.1}$$

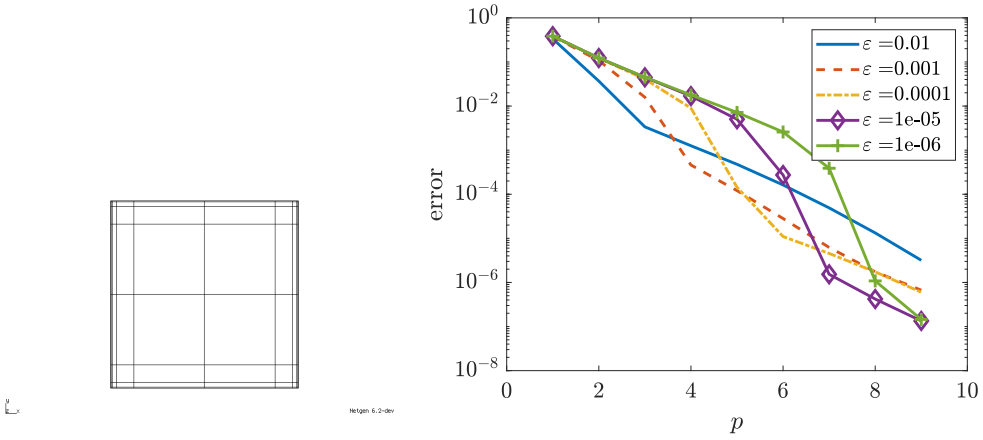

FIG. 8. Right panel: Convergence in the energy norm (5.1) for the square domain for different values of ε and $q = L = n = p$. Left panel: a Netgen-generated mesh used for the computations.

where u_ε^h denotes the discrete solution. In place of the (unknown, for the considered examples) exact solution u_ε we use a numerical approximation on a sufficiently fine mesh. The plots of the estimated numerical errors for the four domains are depicted in Figures 8–11. Evidently, exponential convergence occurs. In agreement with the theoretical analysis, the experimentally observed exponential convergence has two regimes: (i) an asymptotic regime in which the scale resolution condition $\sigma^p \lesssim \varepsilon$ is satisfied and (ii) a pre-asymptotic regime with $\sigma^p \gtrsim \varepsilon$.

The observed exponential convergence in the preasymptotic regime (not rigorously shown in Theorem 4.1) is plausible for the following reason: the approximation error for boundary layer functions is dominated by the error on the elements touching the boundary and is of size $O(\sigma^{p/2})$ for every $p \in \mathbb{N}$. The approximation error of the corner layer functions is likewise dominated by the error on the elements abutting on the vertices of Ω and is of size $O(\sigma^{p(1-\beta)})$ for every $p \in \mathbb{N}$ and some fixed $\beta \in [0,1)$.

5.2 *Fractional Laplacian – a multiscale example*

One of our main motivations in investigating the singularly perturbed reaction diffusion equations is to be able to prove exponential convergence of *hp*-FEM in Ω for spectral fractional diffusion combined with discretized Caffarelli-Silvestre extension or the Balakrishnan representation. For details we refer the reader to Banjai *et al.* (2020). Here we describe how application of a quadrature formula to the Balakrishnan representation leads to a sequence of singularly perturbed problems with a range of scale parameters ε and then apply the *hp*-FEM to each of the problems.

Let $\mathscr{L} := -\nabla \cdot A\nabla$ with A symmetric and uniformly positive definite in $\overline{\Omega}$. We denote by $\{\lambda_k, \varphi_k\}_{k\in\mathbb{N}} \subset \mathbb{R}_{>0} \times H_0^1(\Omega)$ a sequence of eigenpairs of $\mathscr{L}$, normalized such that $\{\varphi_k\}_{k\in\mathbb{N}}$ is an orthonormal basis of

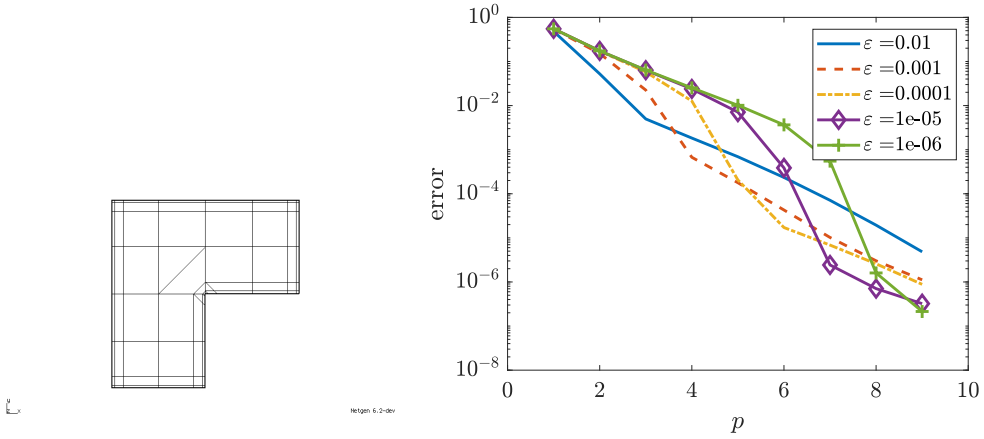

FIG. 9. Right panel: Convergence in the energy norm (5.1) for the L-shaped domain for different values of ε and $q = L = n = p$. Left panel: a Netgen-generated mesh used for the computations.

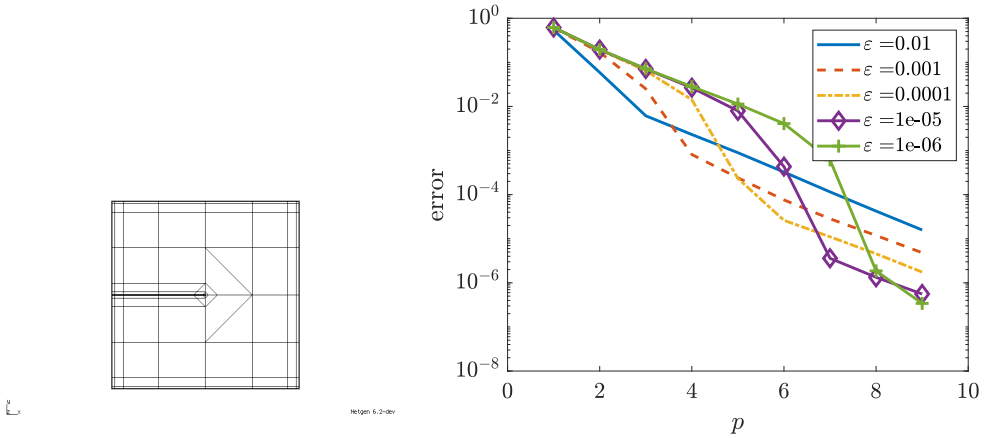

FIG. 10. Right panel: Convergence in the energy norm (5.1) for the slit domain for different values of ε and $q = L = n = p$. Left panel: a Netgen-generated mesh used for the computations.

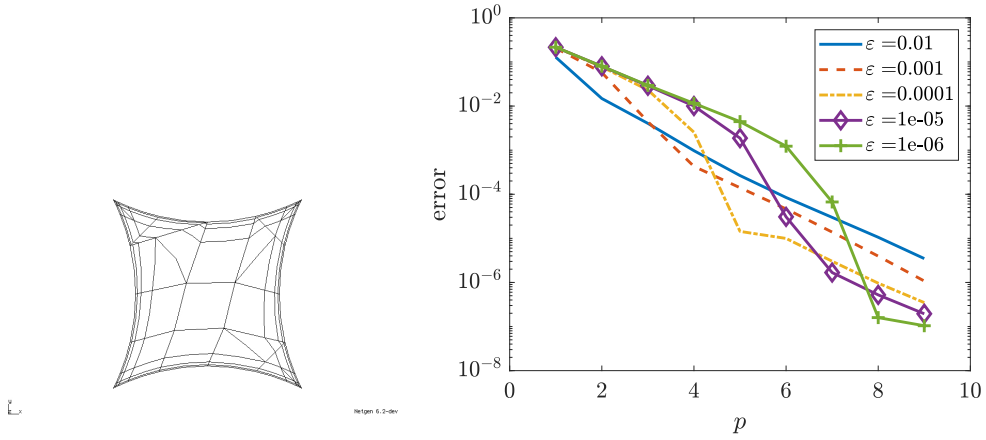

FIG. 11. Right panel: Convergence in the energy norm (5.1) for the domain with curved boundaries for different values of ε and $q = L = n = p$. Left panel: a Netgen-generated mesh used for the computations.

$L^2(\Omega)$ and an orthogonal basis of $H_0^1(\Omega)$ under the respective inner products

$$(u,v)_{L^2(\Omega)} := \int_\Omega u(\mathbf{x})v(\mathbf{x})\,\mathrm{d}\mathbf{x} \quad \text{and} \quad a(u,v) := \int_\Omega A\nabla u(\mathbf{x})\cdot\nabla v(\mathbf{x})\,\mathrm{d}\mathbf{x}.$$

We introduce, for $\sigma \in \mathbb{R}$, the spaces

$$\mathbb{H}^\sigma(\Omega) = \left\{ v = \sum_{k=1}^{\infty} v_k\varphi_k : \|v\|^2_{\mathbb{H}^\sigma(\Omega)} := \sum_{k=1}^{\infty} \lambda_k^\sigma v_k^2 < \infty \right\}. \tag{5.2}$$

For $\sigma > 0$, the spaces $\mathbb{H}^\sigma(\Omega)$ are domain spaces of the fractional powers of $\mathscr{L}$ and $\mathbb{H}^{-\sigma}(\Omega)$ are the corresponding dual spaces. Namely, for $s \in (0,1]$, the spectral fractional operator $\mathscr{L}^s \colon \mathbb{H}^s(\Omega) \to \mathbb{H}^{-s}(\Omega)$ is defined by

$$\mathscr{L}^s v := \sum_{k=1}^{\infty} \lambda_k^s v_k \varphi_k, \qquad \text{for } v \in \mathbb{H}^s(\Omega).$$

The fractional diffusion problem may now be stated as: Given a fractional order $s \in (0,1)$ and $f \in \mathbb{H}^{-s}(\Omega)$, find $u \in \mathbb{H}^s(\Omega)$ such that

$$\mathscr{L}^s u = f \quad \text{in } \Omega\ . \tag{5.3}$$

One approach to this problem going back to Balakrishnan (1960) utilizes the following representation of the solution operator of (5.3):

$$\mathscr{L}^{-s} = \pi^{-1}\sin(\pi s)\int_0^\infty \lambda^{-s}(\lambda I + \mathscr{L})^{-1}\,\mathrm{d}\lambda = \pi^{-1}\sin(\pi s)\int_{-\infty}^{\infty} e^{-sy}(I + e^{-y}\mathscr{L})^{-1}\,\mathrm{d}y. \tag{5.4}$$

In Bonito *et al.* (2019); Bonito & Pasciak (2015) an exponentially convergent, so-called sinc quadrature approximation of (5.4) (see, e.g., Stenger (1993) for details) and an h-version Finite Element projection in Ω was used to obtain numerical approximations of (5.3). The result of the quadrature is the

approximation

$$Q_k^{-s}(\mathscr{L})f := c_B k \sum_{|j|\leqslant K} \varepsilon_j^{2s} \left(I + \varepsilon_j^2 \mathscr{L}\right)^{-1} f, \tag{5.5}$$

where $K \in \mathbb{N}$, $k = K^{-1/2}$, and $\varepsilon_j := e^{-jk/2}$. In (Bonito *et al.*, 2019, Thm. 3.2) it is shown that for $f \in L^2(\Omega)$ and for every $0 \leqslant \beta < s$, $s \in (0,1)$

$$\|(\mathscr{L}^{-s} - Q_k^{-s}(\mathscr{L}))f\|_{\mathbb{H}^{2\beta}(\Omega)} \leqslant C \exp(-b\sqrt{K}) \|f\|_{L^2(\Omega)}$$

for some constants $b, C > 0$ depending on β, s, and Ω.

To produce a fully discrete solution we make use of the hp-FEM with the same space $S_0^p(\Omega, \mathscr{T}_{geo,\sigma}^{p,p})$ for all the $2K+1$ reaction diffusion problems and choose K proportional to p^2. We set $w_j^h \in S_0^p(\Omega, \mathscr{T}_{geo,\sigma}^{p,p})$ to be the solution of

$$\varepsilon_j^2 a(w_j^h, v)_{L^2(\Omega)} + (w_j^h, v)_{L^2(\Omega)} = (f, v)_{L^2(\Omega)}, \qquad \text{for all } v \in S_0^p(\Omega, \mathscr{T}_{geo,\sigma}^{p,p}).$$

The discrete solution of (5.3) is then given by

$$Q_k^{-s}(\mathscr{L}_{hp})f := c_B k \sum_{|j|\leqslant K} \varepsilon_j^{2s} w_j^h.$$

With this choice of hp-FEM space and f analytic on $\overline{\Omega}$, it is shown in Banjai *et al.* (2020) (under the assumption of analyticity of $A(\mathbf{x})$) that for given $c_1 > 0$, there are constants b', $C > 0$ depending on σ and s, such that under the scale condition $\sigma^p \leqslant c_1 e^{-\sqrt{K}/2}$, the error of the full discretization can be bounded as

$$\|\mathscr{L}^{-s} f - Q_k^{-s}(\mathscr{L}_{hp})f\|_{\mathbb{H}^s(\Omega)} \leqslant C \exp(-b' p).$$

Thus, as K is chosen proportional to p^2, the error is $O(e^{-b''\sqrt{K}})$ with $2K+1$ reaction diffusion systems needed to be solved.

We illustrate this result with a numerical example, where we let $\Omega = \Omega_1 = (0,1)^2$ be the unit square from the previous section, $f \equiv 1$, and the diffusion coefficient

$$A(\mathbf{x}) := \begin{cases} \frac{1}{4} & \text{if } (x_1 - \frac{1}{2})(x_2 - \frac{1}{2}) > 0 \\ 4 & \text{otherwise} \end{cases}. \tag{5.6}$$

The diffusion coefficient is discontinuous, thus the problem at hand is beyond the available theory. Nevertheless, the elliptic problems $I + \varepsilon_j^2 \mathscr{L}$ can be expected to have layers at the boundary as well as the lines $x_1 = 1/2$ and $x_2 = 1/2$ and singularities at the vertices of Ω as well as $(1/2, 1/2)$, Kellogg (7475). We will see that exponential convergence is again obtained if additional refinement towards the discontinuity is made. Namely, we again make use of the automatic mesh generation of the NG-Solve/Netgen package Schöberl (1997), but this time also refine towards the lines of discontinuity of A, i.e, for $x_1 = 1/2$ and $x_2 = 1/2$. This automatically provides a geometric refinement towards $(\frac{1}{2}, \frac{1}{2})$, where an algebraic singularity arises. The geometric boundary layer mesh with $L = 4$ refinements and $\sigma = 0.25$ is shown in the left panel of Figure 12. A plot of the solution for $s = 0.2$ is shown on the right of the same figure. It clearly shows the need for the additional refinement.

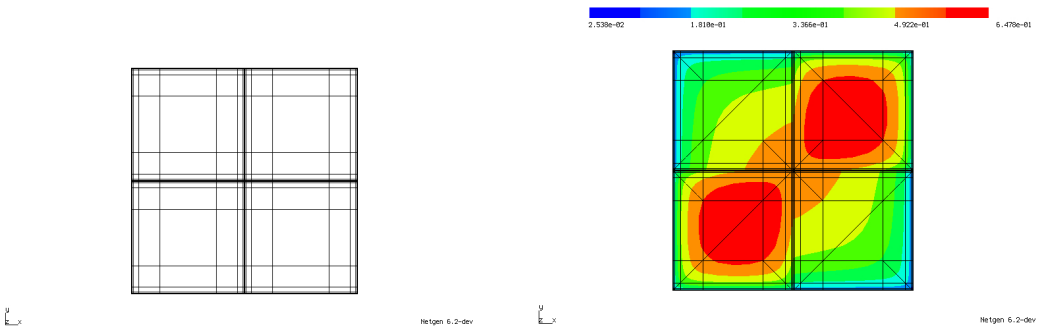

FIG. 12. Left: Netgen generated mesh with geometric refinement towards the boundaries as well as the lines of discontinuity of the diffusion coefficient (5.6). Right: solution of the fractional diffusion problem (5.3) with $s = 0.2$ and diffusion coefficient (5.6).

Instead of using the symmetric approximation (5.5), we follow Bonito *et al.* (2019) and use the refined quadrature rule

$$u_k^h := Q_k^{-s}(\mathscr{L})f := \frac{k\sin(\pi s)}{\pi}\sum_{\ell=-K_1}^{K_2}\varepsilon_j^{2s}(I+\varepsilon_j^2\mathscr{L})^{-1}f, \tag{5.7}$$

with $\varepsilon_j = e^{-jk/2}$ and the number of quadrature points chosen as

$$K_1 = \left\lceil \frac{\pi^2}{2(1-s)k^2} \right\rceil, \qquad K_2 = \left\lceil \frac{\pi^2}{sk^2} \right\rceil;$$

as in Banjai *et al.* (2020), for the given polynomial order $p \geqslant 1$, we set $k = \frac{4}{3}p^{-1}$.

As the exact solution is not available, we make use of a numerical solution on a finer mesh denoted by u^h_{fine} and bound the error in the energy norm (5.1) via the computable right-hand side of the interpolation inequality

$$\|u_k^h - u^h_{\text{fine}}\|_{\mathbb{H}^s(\Omega)} \lesssim \|u_k^h - u^h_{\text{fine}}\|^{1-s}_{L^2(\Omega)} \|u_k^h - u^h_{\text{fine}}\|^{s}_{H^1(\Omega)}.$$

The results of the numerical experiment for $s = 0.2$ and $s = 0.8$ are shown in Figure 13. The exponential convergence against the polynomial order p and $\sqrt{N_{\text{ls}}}$, with N_{ls} being the number of linear systems, illustrates the fact that the fixed hp-FEM space has good approximation properties for reaction diffusion problems with a wide range of parameters $\varepsilon_j = e^{-jk/2}$. For further numerical examples of exponential convergence of this approach, we refer to Banjai *et al.* (2020).

6. Conclusions

We established robust exponential convergence of hp-FEM for solutions of elliptic singular perturbation problems in polygons. These solutions contain, usually, boundary layers, corner singularities and combinations of the two. We admitted possibly multiple length scales, and built the hp-FE approximations on (patches of) geometric boundary layer meshes as described in Section 2, and depicted in Fig. 2. The hp-FEM on this class of partitions is capable to resolve exponential boundary- and corner-layers with

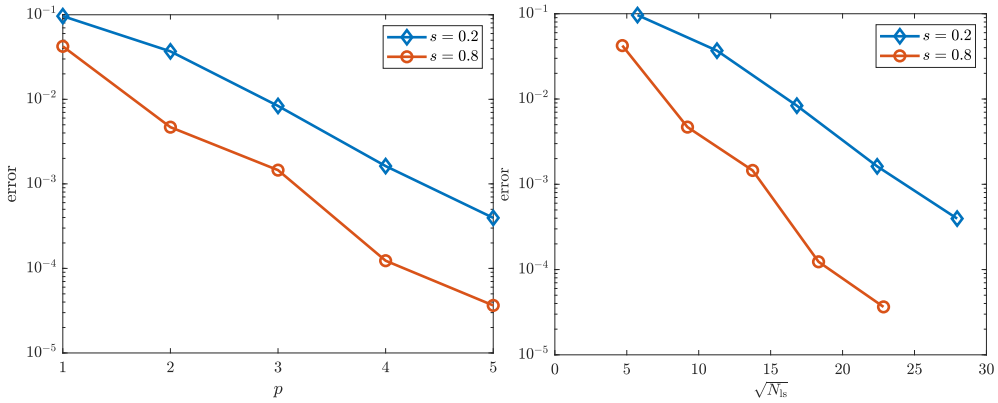

FIG. 13. Convergence in the energy norm (5.1) of the sinc-Balakrishnan, *hp*-FEM discretization for fractional diffusion (5.3) with the discontinuous diffusion coefficient (5.6) on the unit square. On the left panel, the convergence is shown against the polynomial order p and on the right panel against $\sqrt{N_{\rm ls}}$ with $N_{\rm ls}$ the number of reaction diffusion problems solved.

multiple physical length scales under a scale resolution condition that incorporates the smallest physical length scale. The number of geometric mesh refinements to achieve this grows only logarithmically with respect to the smallest length scale. The proposed, spectral numerical boundary layer resolution by *hp*-FEM is based on boundary fitted, structured mesh-patches in the physical domain Ω. They are push-forwards from a finite catalog $\mathfrak{P}$ of canonical, highly structured, anisotropic reference mesh patterns. The key feature of these meshes is the possibly anisotropic geometric refinement towards geometric entities such as corners and edges. Meshes with such properties are available in industrical CAD/CAM environments such as NGSolve Schöberl (1997, 2014). For deployment, it only requires (a lower bound on) the smallest physical length-scale ε. This can often be deduced from heuristic, physical considerations, e.g. scaling or dimensional analysis. The methodology should be contrasted with so-called *"augmented/enriched spectral discretizations"* proposed even recently in Gie *et al.* (2018); Chekroun *et al.* (2020) and in references there. For this numerical approach, *explicit, functional forms of boundary and corner layer components of the solution* are required. The analytic derivation of closed forms for such solution components in general geometries for possibly nonlinear PDEs requires an elaborate asymptotic analysis that may be impossible. It is not necessary in the present approach.

As we explained in the numerical experiments section patch-structured meshes as required here can be generated, in general geometries, by specialized mesh generators such as Netgen Schöberl (1997). We hasten to add, however, that our analysis can readily be extended to cover more general partitions, such as geometric boundary layer meshes that also contain anisotropic triangles.

A focus of the present work was on robust exponential convergence rate bounds for singular perturbation problems in nonsmooth domains by *hp* finite element methods. We proved that they afford robust, exponential convergence on patchwise structured meshes with possibly anisotropic, geometric refinement towards the "support set" (i.e., the subset of $\overline{\Omega}$ off which the layer components decay exponentially), of the boundary and corner layers. As a rule, robust exponential convergence requires genuine *hp*-FE capabilities, i.e., simultaneous mesh refinement and polynomial degree increase, as featured in the *hp*-FE spaces $\{S^p_0(\Omega, \mathscr{T}^{p,p}_{geo,\sigma})\}_{p\geqslant 1}$ used in our numerical experiments. Although we mainly considered the model linear, second order elliptic singular perturbation problem (1.1), corresponding solution families are known to arise for several common models in solid and fluid mechanics, see, e.g.,

Arnold & Falk (1996); Gerdes *et al.* (1998); Chaussade-Beaudouin *et al.* (2017); Gie *et al.* (2018) and the references there.

The present *hp*-error analysis implies exponential upper bounds on Kolmogorov N-widths of solution sets $\{u_\varepsilon : 0 < \varepsilon \leqslant 1\}$ of (1.1). We recall that, for a normed linear space X (with norm $\|\circ\|_X$) and for a subset $B \subset X$, the N-width is given by

$$d_N(B,X) = \inf_{E_N} \sup_{f\in B} \inf_{g\in E_N} \|f-g\|_X, \tag{6.1}$$

where the first infimum is taken over all subspaces E_N of X of dimension $N \in \mathbb{N}$. Subspace sequences $\{E_N\}_{N\geqslant 1}$ which attain the rates of $d_N(B,X)$ in (6.1) can be realized numerically by non-polynomial, so-called *reduced bases* (see Quarteroni *et al.* (2016)).

In (6.1) we choose $(X, \|\circ\|_X) = (H^1_0(\Omega), \|\circ\|_{\varepsilon,\Omega})$ with the energy norm $\|\circ\|_{\varepsilon,\Omega}$ of (1.3). Given a complex neighborhood $G \subset \mathbb{C}^2$ of $\overline{\Omega}$ we take $B \subset X$ as the set of solutions of (1.1) corresponding right-hand sides f that admit a holomorphic extension to G with $\|f\|_{L^\infty(G)} \leqslant 1$. From Corollary 4.1, with $E_N = S^q_0(\Omega, \mathscr{T}^{L,n}_{geo,\sigma})$ we obtain $d_N(B,X) \lesssim \exp(-b\sqrt[4]{N})$ with a continuous, piecewise polynomial interpolant to bound the inner infimum in (6.1). Remark that (Melenk, 2000, Theorem 3.2) stipulates for (1.1) the (sharp) majorization $d_N(A,X) \lesssim \exp(-b'\sqrt{N})$ with $b' > 0$ possibly different from b and with nonpolynomial E_N, but with b' and the constant hidden in $\lesssim$ independent of ε. For analytic $\partial\Omega$ and a single, known boundary layer length scale $\varepsilon \in (0,1]$, this rate is attained by *hp*-FEM on so-called minimal boundary layer meshes (e.g. Schwab *et al.* (1998a); Melenk & Schwab (1998)) which are ε-dependent, however.

The underlying concept of using patchwise structured meshes to approximate parametric solution families to linear, elliptic singularly perturbed boundary value problems extends also to *h*-version FEM. Here, in patches abutting on the boundary analogs of so-called "Shishkin meshes", see, e.g., Shishkin (1987), (Roos *et al.*, 2008, Sec. 3.5.2), could be employed to achieve *robust, algebraic rates of convergence* under weaker, finite order differentiability assumptions on the data A, c, and f than the presently assumed analyticity in $\overline{\Omega}$ of these data. The present results will constitute a foundation for proving exponential convergence of several *hp* discretizations of (spectral) fractional diffusion problems as presented in Banjai *et al.* (2019) in curvilinear polygonal domains Ω. Details will be developed in Banjai *et al.* (2020).

The model problem (1.1) considers homogeneous Dirichlet boundary conditions. The approximation result Theorem 4.1 relies on the regularity results of Melenk (2002), which decomposes the solution (1.1) into boundary and corner layer components. Similar decompositions can be expected to hold also for other boundary conditions. Then the approximation results of Section 3 are applicable indicating that *hp*-FEM on similarly patchwise structured meshes will likewise lead to robust exponential convergence.

A. Analytic changes of variables

The following lemma shows how boundary layer functions are transformed under the patch maps if the edge $\{\widetilde{y} = 0\}$ of $\widetilde{S}$ is mapped to a subset of $\partial\Omega$:

LEMMA A.1 Let $G_x \subset \mathbb{R}\times\mathbb{R}^+$ be a domain. Let the map $M : (\widetilde{x},\widetilde{y}) \mapsto (\theta,\rho)$ be of the form $M(\widetilde{x},\widetilde{y}) = (\breve{\theta}(\widetilde{x},\widetilde{y}), y\breve{\rho}(x,y))$ for some functions $\breve{\theta}$, $\breve{\rho} \geqslant \rho_0 > 0$ that are analytic on closure(G_x), i.e., there are constants $C_M, \gamma_M > 0$ such that $\|\nabla^n\breve{\theta}\|_{L^\infty(G_x)}$, $\|\nabla^n\breve{\rho}\|_{L^\infty(G_x)} \leqslant C_M\gamma_M^n n!$ for all $n \in \mathbb{N}_0$. Let $\mathscr{O}_x \subset G_x$ be open and let $\mathscr{O}$ be an open neighborhood of $M(\mathscr{O}_x)$. Let u be analytic on $\mathscr{O}$ and assume that, for some

function C_u and some constants $b>0$, $\gamma>0$, there holds

$$\forall (m,n)\in\mathbb{N}_0^2 \quad \forall(\rho,\theta)\in\mathscr{O}\colon \ |\partial_\rho^n\partial_\theta^m u(\theta,\rho)|\leqslant C_u(\theta,\rho)e^{-b\rho/\varepsilon}\gamma^{n+m}m!\max\{n,\varepsilon^{-1}\}^n.$$

Then there are constants b', $\widetilde{\gamma}>0$ (depending only on b, γ, and M) such that the function $\widetilde{u}:=u\circ M$ satisfies with the notation $(\rho,\theta)=M(\widetilde{x},\widetilde{y})$

$$\forall (m,n)\in\mathbb{N}_0^2 \quad \forall(\widetilde{x},\widetilde{y})\in\mathscr{O}_x\colon \ |\partial_{\widetilde{y}}^n\partial_{\widetilde{x}}^m \widetilde{u}(\widetilde{x},\widetilde{y})|\leqslant C_u(\theta,\rho)e^{-b'\widetilde{y}/\varepsilon}\gamma^{n+m}m!\max\{n,\varepsilon^{-1}\}^n.$$

Proof. The proof uses arguments employed in (Melenk, 2002, Sec. 4.3). Consider a fixed $(\widetilde{x},\widetilde{y})\in\mathscr{O}_x$ and set $(\theta',\rho')=M(\widetilde{x},\widetilde{y})$. Then $(\theta,\rho)\mapsto u(\theta,\rho)$ is holomorphic on the polydisc

$$B_{1/\gamma}(\theta')\times B_{1/(\gamma e)}(\rho')\subset\mathbb{C}^2$$

with the bound

$$|u(\theta'+\zeta_1,\rho'+\zeta_2)|\leqslant C_u(\rho',\theta')e^{-b\rho'/\varepsilon}\frac{1}{1-\gamma|\zeta_1|}\left[\frac{1}{1-\gamma e|\zeta_2|}+\exp\left(\gamma|\zeta_2|/\varepsilon\right)\right]. \tag{A.1}$$

Since the functions $\check{\theta}$, $\check{\rho}$ are holomorphic on the closure of $M(G_x)$, there are C_1, $\delta>0$ (independent of $(\widetilde{x},\widetilde{y})\in G$) such that for ζ_1, $\zeta_2\in B_\delta(0)\subset\mathbb{C}$ there holds

$$\begin{aligned}\left|\check{\theta}(\widetilde{x}+\zeta_1,y+\zeta_2)-\check{\theta}(\widetilde{x},\widetilde{y})\right|&\leqslant C_1\left[|\zeta_1|+|\zeta_2|\right],\\ |(\widetilde{y}+\zeta_2)\check{\rho}(\widetilde{x}+\zeta_1,\widetilde{y}+\zeta_2)-\widetilde{y}\check{\rho}(\widetilde{x},\widetilde{y})|&\leqslant C_1\left[y(|\zeta_1|+|\zeta_2|)+|\zeta_2|\right],\end{aligned}$$

and we may assume that $\delta>0$ is such that for ζ_1, $\zeta_2\in B_\delta(0)$ we have $M(\widetilde{x}+\zeta_1,\widetilde{y}+\zeta_2)\in B_{1/(2\gamma)}(\theta')\times B_{1/(2\gamma e)}(\rho')$. This implies in view of (A.1) the bounds

$$\begin{aligned}|\widetilde{u}(\widetilde{x}+\zeta_1,\widetilde{y}+\zeta_2)|&=|u(M(\widetilde{x}+\zeta_1,\widetilde{y}+\zeta_2))| &\text{(A.2)}\\ &\leqslant CC_u(\theta',\rho')e^{-b\rho'/\varepsilon}\exp(C_1\gamma|\zeta_2|/\varepsilon)\exp\big(C_1\gamma\widetilde{y}\left[|\zeta_1|+|\zeta_2|\right]/\varepsilon\big). &\text{(A.3)}\end{aligned}$$

For δ_1, $\delta_2<\delta$ Cauchy's integral formula for derivatives gives

$$\partial_{\widetilde{x}}^{\alpha_1}\partial_{\widetilde{y}}^{\alpha_2}\widetilde{u}(\widetilde{x},\widetilde{y})=-\frac{\alpha_1!\alpha_2!}{4\pi^2}\int_{\zeta_1\in\partial B_{\delta_1}(0)}\int_{\zeta_2\in\partial B_{\delta_2}(0)}\frac{\widetilde{u}(x+\zeta_1,y+\zeta_2)}{(-\zeta_1)^{\alpha_1+1}(-\zeta_2)^{\alpha_2+1}}\,d\zeta_1 d\zeta_2$$

so that

$$\left|\partial_{\widetilde{x}}^{\alpha_1}\partial_{\widetilde{y}}^{\alpha_2}\widetilde{u}(\widetilde{x},\widetilde{y})\right|\leqslant CC_u(\rho',\theta')e^{-b\rho'/\varepsilon}\frac{\alpha_1!}{\delta_1^{\alpha_1}}\frac{\alpha_2!}{\delta_2^{\alpha_2}}\exp(C_1\gamma\delta_2/\varepsilon)\exp(C_1\gamma y(\delta_1+\delta_2)/\varepsilon)$$

Selecting $\delta_1=\delta:=b\rho_0/(4C_1)$ and $\delta_2=\min\{(|\alpha_2|+1)\varepsilon,\delta\}$ yields the desired result with $b'=b/2$ since $C_1\widetilde{y}(\delta_1+\delta_2)/\varepsilon\leqslant 2\delta C_1\widetilde{y}/\varepsilon\leqslant 2\delta C_1\rho'/\rho_0=b/2$. □

The following lemma shows how functions that may have a singular behavior are transformed under analytic changes of variables:

LEMMA A.2 ((Melenk, 2002, Lemma 4.3.3)) Let $\widetilde{G}\subset\mathbb{R}^2$ be a domain and $M:\widetilde{G}\to\mathbb{R}^2$ be analytic on closure($\widetilde{G}$). Let $\widetilde{\mathscr{O}}\subset\widetilde{G}$ be open and $\mathscr{O}$ be an open neighborhood of $M(\widetilde{\mathscr{O}})$. Let u be analytic on $\mathscr{O}$ and assume that for some (positive) function Λ, $r:\mathscr{O}\to\mathbb{R}$ and some $\gamma\geqslant 0$ there holds

$$\forall n\in\mathbb{N}_0 \quad \forall\mathbf{x}\in\mathscr{O}\colon \ |\nabla^n u(\mathbf{x})|\leqslant\Lambda(\mathbf{x})\gamma^n\max\{(n+1)/r(\mathbf{x}),\varepsilon^{-1}\}^n. \tag{A.4}$$

Then the function $\widetilde{u} := u \circ M$ is analytic on $\widetilde{\mathscr{O}}$ and there are constants C, $\widetilde{\gamma} > 0$ depending solely on M and γ such that for each $\widetilde{\mathbf{x}} \in \widetilde{\mathscr{O}}$ there holds with the notation $\mathbf{x} = M(\widetilde{\mathbf{x}})$

$$\forall n \in \mathbb{N}_0 \colon \quad |\nabla^n \widetilde{u}(\widetilde{\mathbf{x}})| \leqslant C\Lambda(\mathbf{x})\widetilde{\gamma}^n \max\{(n+1)/r(\mathbf{x}), \varepsilon^{-1}\}^n.$$

Proof. The statement is taken from (Melenk, 2002, Lemma 4.3.3) except that we explicitly allow r to be a function of $\mathbf{x}$. The proof is similar to that of Lemma A.1. We fix $\widetilde{\mathbf{x}} \in \widetilde{G}$ and set $\mathbf{x} = M(\widetilde{\mathbf{x}})$. The assumption (A.4) implies that u has a holomorphic extension to $B_{cr(\mathbf{x})}(\mathbf{x}) \subset \mathbb{C}^2$ with $c > 0$ depending solely on γ. Additionally, we have the bound for $z \in B_{cr(\mathbf{x})}(\mathbf{x}) \subset \mathbb{C}^2$ (we write $r = r(\mathbf{x})$)

$$|u(\mathbf{x}+z)| \leqslant \Lambda(\mathbf{x}) \sum_{n=0}^{\infty} \frac{1}{n!}|z|^n |\nabla^n u(\mathbf{x})| \leqslant C\left[\frac{1}{1-|z|/(cr)} + \exp(C'|z|/\varepsilon)\right].$$

for suitable C, C'. The analyticity of M on closure$(\widetilde{G})$ implies the existence of $\delta > 0$ (independent of $\widetilde{\mathbf{x}} = (\widetilde{x}, \widetilde{y}) \in \widetilde{G}$) such that

$$M(\widetilde{x} + B_{\delta r}(0), \widetilde{y} + B_{\delta r}(0)) \subset B_{\frac{1}{2}cr(\mathbf{x})}(\mathbf{x}).$$

For $\alpha \in \mathbb{N}_0^2$ let $\theta := \min\{\delta r(\mathbf{x}), (|\alpha|+1)\varepsilon\}$. The Cauchy integral theorem for derivatives gives

$$\partial_{\widetilde{x}}^{\alpha_1} \partial_{\widetilde{y}}^{\alpha_2} \widetilde{u}(\widetilde{x}, \widetilde{y}) = -\frac{\alpha_1! \alpha_2!}{4\pi^2} \int_{z_1 \in \partial B_\theta(0)} \int_{z_2 \in \partial B_\theta(0)} \frac{\widetilde{u}(M(\widetilde{\mathbf{x}} + (z_1, z_2)))}{(-z_1)^{\alpha_1+1}(-z_2)^{\alpha_2+1}}$$

so that we get

$$\begin{aligned} |\partial_{\widetilde{x}}^{\alpha_1} \partial_{\widetilde{y}}^{\alpha_2} \widetilde{u}(\widetilde{x}, \widetilde{y})| &\lesssim \alpha_1! \alpha_2! \theta^{-|\alpha|} \left[1 + \exp(C'\theta/\varepsilon)\right] \\ &\lesssim |\alpha|! \max\{(\delta r(\mathbf{x}))^{-1}, (|\alpha|+1)^{-1}\varepsilon^{-1}\}^{|\alpha|} \left[1 + \exp(C'|\alpha|)\right], \end{aligned}$$

which proves the asserted estimate. □

B. Univariate Approximation

LEMMA A.1 Let $I = (-1, 1)$ and $u \in C^\infty(I)$ satisfy, for some constants C_u, $\gamma_u > 0$, for some $h \in (0, 1]$, $\varepsilon \in (0, 1]$ the bound

$$\forall n \in \mathbb{N}_0 \colon \quad \|D^n u\|_{L^\infty(I)} \leqslant C_u(\gamma_u h)^n \max\{n, \varepsilon^{-1}\}^n. \tag{A.1}$$

Then there are constants C, η, $\delta > 0$ depending solely on γ_u such that under the constraint

$$\frac{h}{\varepsilon q} \leqslant \delta \tag{A.2}$$

there holds

$$\forall q \in \mathbb{N} \colon \quad \inf_{v \in \mathbb{P}_q} \|u - v\|_{W^{1,\infty}(I)} \leqslant CC_u \left(\left(\frac{h}{h+\eta}\right)^{q+1} + \left(\frac{h}{\eta\varepsilon q}\right)^{q+1} \right). \tag{A.3}$$

Proof. We start with the observation that Taylor's theorem yields for $x > 0$

$$\sum_{n \geqslant q+1} \frac{1}{n!} x^n = e^x - \sum_{n=0}^{q} \frac{x^n}{n!} = \frac{1}{q!} \int_0^x (x-t)^q e^t \, dt \leqslant \frac{x^{q+1}}{q!} e^x. \tag{A.4}$$

Case 1: Let $e\gamma_u h < 1/2$. Then the Taylor series of u about $x_0 = 0$ converges in I and the Taylor polyomials $T_q \in \mathbb{P}_q$ satisfy the error bounds

$$\begin{aligned}\|u - T_q\|_{L^\infty(I)} &\leqslant \sum_{n=q+1}^{\infty} \frac{|D^n u(0)|}{n!} \leqslant C_u \sum_{n=q+1}^{\infty} (\gamma_u e h)^n + \frac{(\gamma_u h/\varepsilon)^n}{n!} \\ &\overset{(A.4)}{\leqslant} C_u \left(\frac{(\gamma_u e h)^{q+1}}{1-(\gamma_u e h)} + \frac{(\gamma_u h/\varepsilon)^{q+1}}{q!} e^{\gamma_u h/\varepsilon} \right) \\ &\overset{(A.8)}{\leqslant} C_u \left(2(\gamma_u e h)^{q+1} + C(\gamma' h/(\varepsilon q))^{q+1} e^{\gamma_u h/\varepsilon} \right),\end{aligned}$$

for suitable $\gamma' > \gamma_u$. The assumption (A.2) allows us to estimate $e^{\gamma_u h/\varepsilon} \leqslant e^{\gamma_u \delta q}$ and the desired result follows for the L^∞-estimate. An analogous argument applies for the $W^{1,\infty}$-estimate.

Case 2: Let $1 \geqslant h > 1/(2e\gamma_u)$. Introduce for $\rho > 1$ the ellipse $\mathscr{E}_\rho := \{z \in \mathbb{C} \,|\, |z-1| + |z+1| < \rho + 1/\rho\}$ and set $G_\kappa(I) := \cup_{x \in I} B_\kappa(x)$. By geometric considerations (e.g., with the aid of (Börm *et al.*, 2005, Lemma 3.14)) one has $\mathscr{E}_{1+\kappa} \subset G_\kappa(I)$. Taylor's theorem gives that u is holomorphic on $G_{1/(\gamma_u h)}(I)$ and for every $\kappa < 1/(\gamma_u h)$ we have

$$\|u\|_{L^\infty(G_\kappa)} \leqslant C_u \sum_{n=0}^{\infty} \frac{1}{n!} (h\gamma_u \kappa)^n \max\{n, \varepsilon^{-1}\}^n \leqslant C_u \left[\frac{1}{1 - e\gamma_u h \kappa} + \exp(\kappa \gamma_u h/\varepsilon) \right]. \tag{A.5}$$

Well-established polynomial approximation results (see, e.g., (Apel & Melenk, 2018, Thm. 6)) then yield for fixed $\kappa > 0$ the existence of $\rho_1 = \rho_1(\kappa) > 1$ such that

$$\inf_{v \in \mathbb{P}_q} \|u - v\|_{W^{1,\infty}(I)} \leqslant C C_u \rho_1^{-q} \|u\|_{L^\infty(G_\kappa)} \leqslant C C_u \rho_1^{-q} e^{\kappa \gamma_u h/\varepsilon} \leqslant C C_u \rho_1^{-q} e^{\kappa \gamma_u \delta q}.$$

Fix $1 < \rho_2 < \rho_1$. Then we may select $\delta > 0$ sufficiently small so that there exists a constant $C > 0$ such that

$$\forall q \in \mathbb{N}: \quad \inf_{v \in \mathbb{P}_q} \|u - v\|_{W^{1,\infty}(I)} \leqslant C C_u \rho_2^{-q}.$$

Using $h \geqslant 1/(2e\gamma_u)$ and suitably choosing η, we can estimate

$$\rho_2^{-q} \leqslant \left(\frac{h}{h+\eta} \right)^q.$$

□

LEMMA A.2 (stability of the 1d-Gauss-Lobatto (GL) interpolant) Let $I = [-1,1]$. There exists a constant $C > 0$ such that for any $q \in \mathbb{N}$, the Gauss-Lobatto interpolation operator $i_q : C^0(I) \to \mathbb{P}_q$ satisfies:

$$\|u - i_q u\|_{L^\infty(I)} \leqslant (1 + \Lambda_q) \inf_{v \in \mathbb{P}_q} \|u - v\|_{L^\infty(I)}, \qquad \Lambda_q = C \ln(q+1), \tag{A.6}$$

$$\|(u - i_q u)'\|_{L^\infty(I)} \leqslant C^0 (1 + q^2 \Lambda_q) \inf_{v \in \mathbb{P}_q} \|(u - v)'\|_{L^\infty(I)}. \tag{A.7}$$

Proof. The bound (A.6) follows from the projection property of the Gauss-Lobatto interpolation; the logarithmic growth of the Lebesgue constant Λ_q is shown in Sündermann (1983).

For (A.7), we estimate for arbitrary $v \in \mathbb{P}_q$

$$\begin{aligned}\|(u-i_q u)'\|_{L^\infty(I)} &\leqslant \|(u-v)'\|_{L^\infty(I)} + \|(i_q(u-v))'\|_{L^\infty(I)} \\ &\lesssim \|(u-v)'\|_{L^\infty(I)} + q^2\|i_q(u-v)\|_{L^\infty(I)} \lesssim \|(u-v)'\|_{L^\infty(I)} + q^2\Lambda_q\|u-v\|_{L^\infty(I)}.\end{aligned}$$

Constraining v to satisfy $v(-1) = u(-1)$ the result follows from a Poincaré inequality. □ Finally, we recall two inequalities of Stirling's type.

$$\forall n \in \mathbb{N}: \quad \sqrt{2\pi}n^{n+1/2}e^{-n} \leqslant n! \leqslant en^{n+1/2}e^{-n}\,, \tag{A.8}$$

$$\forall n \in \mathbb{N}_0 \quad \forall \alpha \in \mathbb{N}_0: \quad \alpha! n! \geqslant 2^{-(\alpha+n)}(\alpha+n)! \geqslant (2e)^{-(\alpha+n)}(\alpha+n)^{\alpha+n}. \tag{A.9}$$

(A.8) follows from Robbins (1955). In A.9, the first bound follows from the binomial formula $\sum_{\nu=0}^{m}\binom{m}{\nu}x^\nu = (1+x)^m$ and the second bound follows from (A.8).

REFERENCES

APEL, T. & MELENK, J. (2018) Interpolation and quasi-interpolation in *h*- and *hp*-version finite element spaces. *Encyclopedia of Computational Mechanics* (E. Stein, R. de Borst & T. Hughes eds). Chichester, UK: John Wiley & Sons, pp. 1–33. extended preprint at `http://www.asc.tuwien.ac.at/preprint/2015/asc39x2015.pdf`.

ARNOLD, D. N. & FALK, R. S. (1996) Asymptotic analysis of the boundary layer for the Reissner-Mindlin plate model. *SIAM J. Math. Anal.*, **27**, 486–514.

BABUŠKA, I. & GUO, B. (1986a) The $h-p$ version of the finite element method. Part 1: The basic approximation results. *Computational Mechanics*, **1**, 21–41.

BABUŠKA, I. & GUO, B. (1986b) The $h-p$ version of the finite element method. Part 2: General results and applications. *Computational Mechanics*, **1**, 203–220.

BABUŠKA, I. & GUO, B. (1988) The *h*-*p* version of the finite element method for domains with curved boundaries. *SIAM J. Numer. Anal.*, **25**, 837–861.

BALAKRISHNAN, A. V. (1960) Fractional powers of closed operators and the semigroups generated by them. *Pacific J. Math.*, **10**, 419–437.

BANJAI, L., MELENK, J. M., NOCHETTO, R. H., OTÁROLA, E., SALGADO, A. J. & SCHWAB, C. (2019) Tensor FEM for spectral fractional diffusion. *Found. Comput. Math.*, **19**, 901–962.

BANJAI, L., MELENK, J. M. & SCHWAB, C. (2020) Exponential Convergence of *hp*-FEM for Spectral Fractional Diffusion in Polygons. arXiv:2011.05701.

BONITO, A., LEI, W. & PASCIAK, J. E. (2019) On sinc quadrature approximations of fractional powers of regularly accretive operators. *J. Num. Math.*, **27**, 57–68.

BONITO, A. & PASCIAK, J. (2015) Numerical approximation of fractional powers of elliptic operators. *Math. Comp.*, **84**, 2083–2110.

BÖRM, S., LÖHNDORF, M. & MELENK, J. M. (2005) Approximation of integral operators by variable-order interpolation. *Numer. Math.*, **99**, 605–643.

BURET, F., DAUGE, M., DULAR, P., KRÄHENBÜHL, L., PÉRON, V., PERRUSSEL, R., POIGNARD, C. & VOYER, D. (2012) Eddy currents and corner singularities. *IEEE Transactions on Magnetics*, **48**, 679–68.

CHAUSSADE-BEAUDOUIN, M., DAUGE, M., FAOU, E. & YOSIBASH, Z. (2017) Free vibrations of axisymmetric shells: parabolic and elliptic cases. *Asymptot. Anal.*, **104**, 1–47.

CHEKROUN, M. D., HONG, Y. & TEMAM, R. M. (2020) Enriched numerical scheme for singularly perturbed barotropic quasi-geostrophic equations. *J. Comput. Phys.*, **416**, 109493, 28.

FAUSTMANN, M. & MELENK, J. M. (2017) Robust exponential convergence of *hp*-FEM in balanced norms for singularly perturbed reaction-diffusion problems: corner domains. *Comput. Math. Appl.*, **74**, 1576–1589.

GERDES, K., MATACHE, A. M. & SCHWAB, C. (1998) Analysis of membrane locking in *hp* FEM for a cylindrical shell. *ZAMM Z. Angew. Math. Mech.*, **78**, 663–686.

GIE, G.-M., HAMOUDA, M., JUNG, C.-Y. & TEMAM, R. M. (2018) *Singular perturbations and boundary layers*. Applied Mathematical Sciences, vol. 200. Springer, Cham, pp. xviii+412.

KELLOGG, R. B. (1974/75) On the Poisson equation with intersecting interfaces. *Applicable Anal.*, **4**, 101–129.

MELENK, J. (1997) A note on robust exponential convergence of finite element methods for problems with boundary layers. *IMA Journal of Numerical Analysis*, **17**, 557–601.

MELENK, J. (2002) *hp-finite element methods for singular perturbations*. Lecture Notes in Mathematics, vol. 1796. Springer-Verlag, Berlin, pp. xiv+318.

MELENK, J. M. (2000) On n-widths for elliptic problems. *J. Math. Anal. Appl.*, **247**, 272–289.

MELENK, J. M. & RIEDER, A. (2021) *hp*-FEM for the fractional heat equation. *IMA J. Numer. Anal.*, **41**, 412–454.

MELENK, J. M. & SAUTER, S. (2010) Convergence analysis for finite element discretizations of the Helmholtz equation with Dirichlet-to-Neumann boundary conditions. *Math. Comp.*, **79**, 1871–1914.

MELENK, J. M. & XENOPHONTOS, C. (2016) Robust exponential convergence of *hp*-FEM in balanced norms for singularly perturbed reaction-diffusion equations. *Calcolo*, **53**, 105–132.

MELENK, J. & SCHWAB, C. (1998) *hp* FEM for reaction-diffusion equations. I. Robust exponential convergence. *SIAM J. Numer. Anal.*, **35**, 1520–1557.

MELENK, J. & SCHWAB, C. (1999) An *hp* finite element method for convection-diffusion problems in one dimension. *IMA Journal of Numerical Analysis*, **19**, 425–453.

QUARTERONI, A., MANZONI, A. & NEGRI, F. (2016) *Reduced basis methods for partial differential equations*. Unitext, vol. 92. Springer, Cham, pp. xi+296. An introduction, La Matematica per il 3+2.

ROBBINS, H. (1955) A remark on Stirling's formula. *Amer. Math. Monthly*, **62**, 26–29.

ROOS, H.-G., STYNES, M. & TOBISKA, L. (2008) *Robust numerical methods for singularly perturbed differential equations*. Springer Series in Computational Mathematics, vol. 24, second edn. Springer-Verlag, Berlin, pp. xiv+604. Convection-diffusion-reaction and flow problems.

SCHÖBERL, J. (1997) Netgen an advancing front 2d/3d-mesh generator based on abstract rules. *J. Comput. Visual. Sci.*, **1**, 41–52.

SCHÖBERL, J. (2014) C++11 implementation of finite elements in NGSolve. *Technical Report*. Institute for Analysis and Scientific Computing, Vienna University of Technology.

SCHWAB, C., SURI, M. & XENOPHONTOS, C. (1998a) The *hp* Finite Element Method for problems in mechanics with boundary layers. *Comp. Meth. Appl. Mech. Engg.*, **157**, 311–333.

SCHWAB, C., SURI, M. & XENOPHONTOS, C. (1998b) The *hp* finite element method for problems in mechanics with boundary layers. *Comput. Methods Appl. Mech. Engrg.*, **157**, 311–333. Seventh Conference on Numerical Methods and Computational Mechanics in Science and Engineering (NMCM 96) (Miskolc).

SCHWAB, C. (1998) *p- and hp-Finite Element Methods*. Numerical Mathematics and Scientific Computation. The Clarendon Press, Oxford University Press, New York, pp. xii+374. Theory and applications in solid and fluid mechanics.

SCHWAB, C. & SURI, M. (1996) The *p* and *hp* versions of the finite element method for problems with boundary layers. *Math. Comp.*, **65**, 1403–1429.

SHISHKIN, G. I. (1987) Approximation of solutions of singularly perturbed boundary value problems with a corner boundary layer. *Zh. Vychisl. Mat. i Mat. Fiz.*, **27**, 1360–1374, 1438.

STENGER, F. (1993) *Numerical methods based on sinc and analytic functions*. Springer Series in Computational Mathematics, vol. 20. Springer-Verlag, New York, pp. xvi+565.

SÜNDERMANN, B. (1983) Lebesgue constants in Lagrangian interpolation at the Fekete points. *Mitt. Math. Ges. Hamb.*, **11**, 204–211.